Table of Contents

Please see below for respective responses to three reviewers. Our responses are in blue. The figures and equations in each chapter are labeled separately. The line numbers below are those from the revised manuscript with tracking changes.

1. Reviewer#1

This study showed a close spatio-temporal covariability between biogeochemical module based on CoSINE model and kinetic energy based on ocean current from ADT in summer Vietnam upwelling system. The model results show that weakened circulation and eddy activity, with ~21% less nitrate inventory and ~16% weaker primary productivity when separation current is absent.
My impression on this manuscript is that two different physical and biological perspectives are well linked together to address productivity changes in response to physical forces. However, I found some misleading facts from the results that this paper discussed. Thus, I would like to recommend to accept this paper for the publication of OS after some revision.

We appreciate the positive feedbacks from the referee. Please see point-by-point responses below.

Major Comments:

1. **Is there any critical condition to explain that the elevated kinetic energy and intensified circulation can be explained by the separation of the upwelling current system (as described in Abstract).**

It is a good point to further quantify the flow separation. Additional discussion was added to Appendix B. We also revised this sentence to make it clearer: “the elevated kinetic energy is linked to the strength of the current separation from the coast.”
Appendix B as below:
“Qualitatively, both the analysis based on remote sensing data and model results suggest the separation flow is linked with stronger KE (~65% larger in HNA case then LNA case, Sect. 3.1). Moreover, a separation index is defined to quantitatively explain the relation between the flow separation and intensified circulation. The separation index (SI) can be written as:

$$SI = \sum \frac{u \cdot \cos\varphi + v \cdot \sin\varphi}{\sqrt{u^2 + v^2}}, \qquad \text{(S1)}$$

where u and v are the two surface velocity components, and φ is the angle between the topography gradient and the positive x axis. This SI is essentially the area-averaged cross-isobath velocity normalized by the magnitude of the velocity, which is used to quantify flow separation here.

Fig. S1 shows the distribution of SI in Aug 2010. Positive values indicate that the flow is separating and downslope, and that may be seen off Vietnam south of the coastline bend. Large SI (~1.0) can be observed near the separation point ~11.5°N. Taking spatial average over the box region in Fig. 2a or Fig. S1, there is a good positive correlation (R=0.7175, p<0.01) between log(KE) and SI (see Fig. S2). Moreover, SI may be seen to generally increase with KE to a value of 0.25~0.3 and then it levels off (i.e. the slope becomes less) – see the red and blue lines in Fig. S2. The log(KE) and SI thus appears to show a logistic-type behavior, in which SI asymptotically approaches some maximum value (in this case ~0.3). This suggest that the strong flow separation and elevated KE are tightly linked. From Fig. S2, the value of KE ≈ 0.1 m^2s^{-2} appears to be a critical value.

Dynamically, the nonlinear advection term in the momentum equation can be written as the vector invariant form [see e.g., Gill (1982)]:

$$\vec{u} \cdot \nabla \vec{u} = (\nabla \times \vec{u}) \times \vec{u} + \nabla\left(\frac{1}{2}\left|\vec{u}\right|^2\right)$$

This decomposition directly links the nonlinear advection term and the gradient of KE (which scales KE over a length scale L). Meanwhile, the nonlinear advection is an important mechanism in driving flow separation [see, for instance, Oey et al. (2014)]. Stronger advection suggests intense cross isobath flow. Therefore, a dynamic linkage between the flow separation and the intensified KE and circulation can also be established, further supporting this argument.

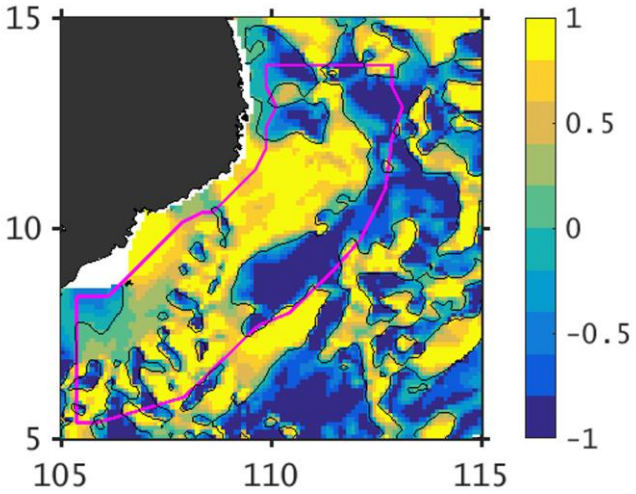

Figure S1 Example of modeled SI in Aug 2010.

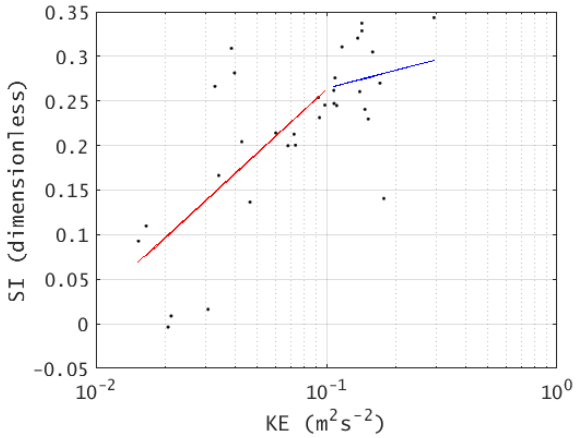

Figure S2 Summer-month (MJJAS) KE vs SI averaged over the box region in Fig. S2 (overall R=0.7175).

2. Authors discuss Figure 5 for model comparison with OISST and VGPM NPP. To me, model SST and NPP are not quite similar. Although authors admit its discrepancies, authors need to estimate this SST differences can cause how much uncertainties to obtain the result from covariability in physical-biological interaction.

Thank you for this comment. We agree that the modeled and observed patterns did not match so well. However, while it is true that SST affects NPP through, for example, changes in the vertical stratification of the water column, both SST and NPP strongly depend on circulation (e.g. upwelling and/or downwelling), and in our case on the flow separation and KE also. In turn, the circulation is dominated by changes in the upper-layer depth (as diagnosed through the SSH) and the horizontal gradients of SSH, and is much less dependent on the gradients of SST. Thus, the co-variation between the SST and ecosystem is largely controlled by the circulation, as discussed in the manuscript.

The dominant ecosystem response is the separation and non-separation contrast, which is captured well by the model (compare Fig. 4 and Fig. 8).
Discussion on this point was added to Line 250 through 258.

3. For Fig. 7 (Line 218), "Subsurface CHL maxima appears at ~35 m, which is somewhat shallower than that in the observation." Authors also need to discuss this depth differences leading to how much uncertainties to obtain current results.

Discussion was added in Line 276:
"Except for model uncertainty, this discrepancy may be also related with the undersampling in observed profiles (no water samples between 25 m and 50 m depth). When CHL is considered as a proxy of the production, vertical-integrated CHL is more relevant. The vertical-averaged (5 m to 150 m) CHL in the model and observation are 0.1595 and 0.1668 mg m^{-3}, respectively, which have a marginal difference (< 5%)."
Mean observation profiles were also added to Fig. 7, as the black profiles below.

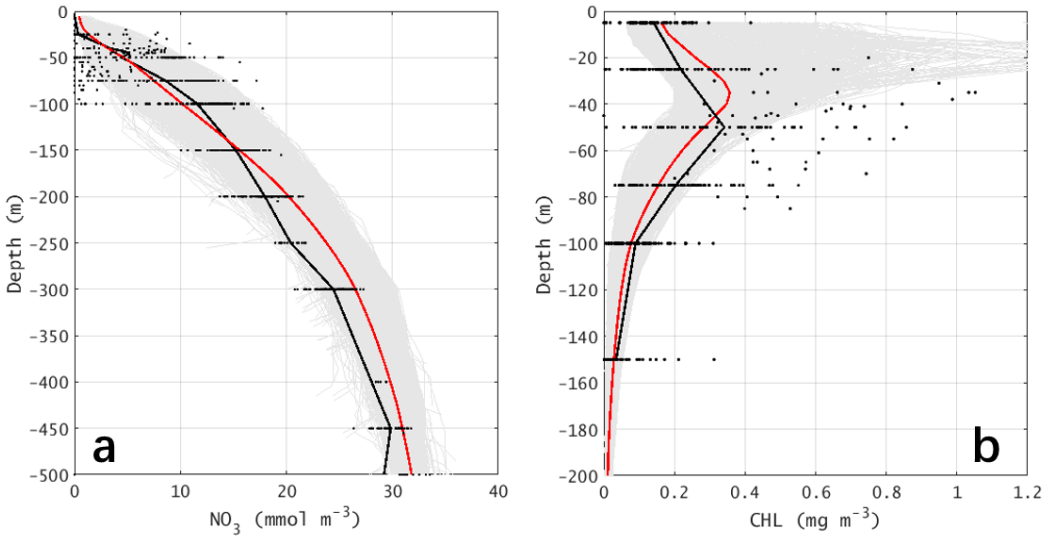

Minor Comments
Fig. 1, Magenta diamonds for observation stations are not clear. Change them with
another better color (maybe black color)
Sure. Black color looks good as now they are in.

Fig.2 shows CHL concentraton in Fig. 2a. I am wondering whether its magnitudes are right. It seems too low. Authors need to check.
In Fig. 2a, the averaged CHL value in the summer VBUS is ~0.15 offshore and >0.45 nearshore. These values are consistent with the values from literature, for instance (Fig. S3), Loisel et al. (2017). Noting that in Fig. 2a the nearshore CHL can be as large as 5.0 mg m^{-3} exceeding the color scale, we replaced the color scale with a log2 scale (Fig.

S4 and revised Fig. 2).

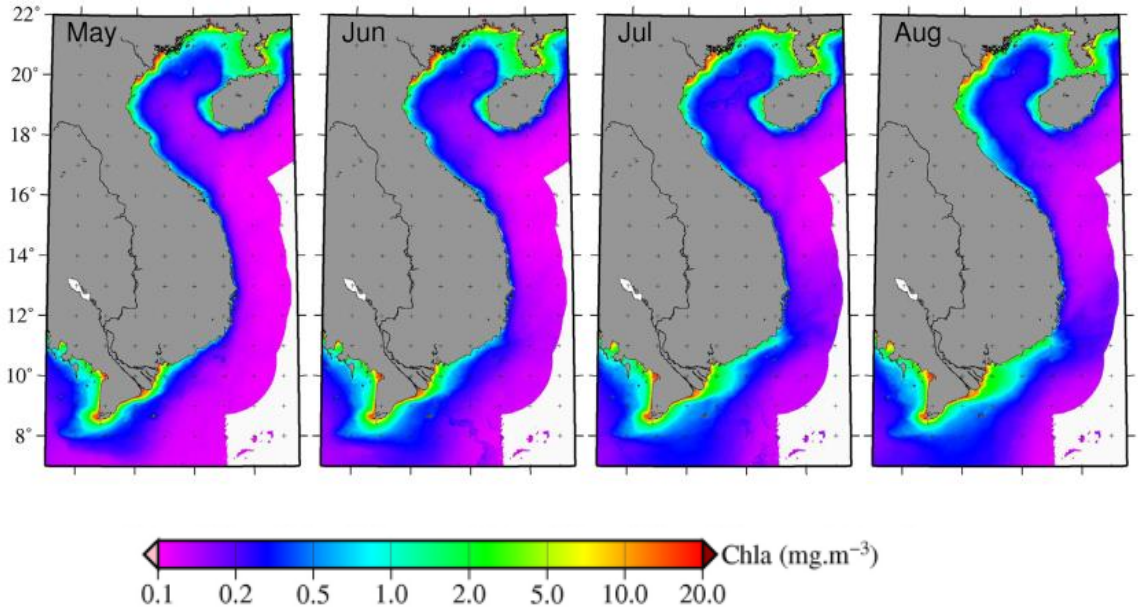

Figure S3 Climatological monthly CHL concentration from Loisel et al. (2017).

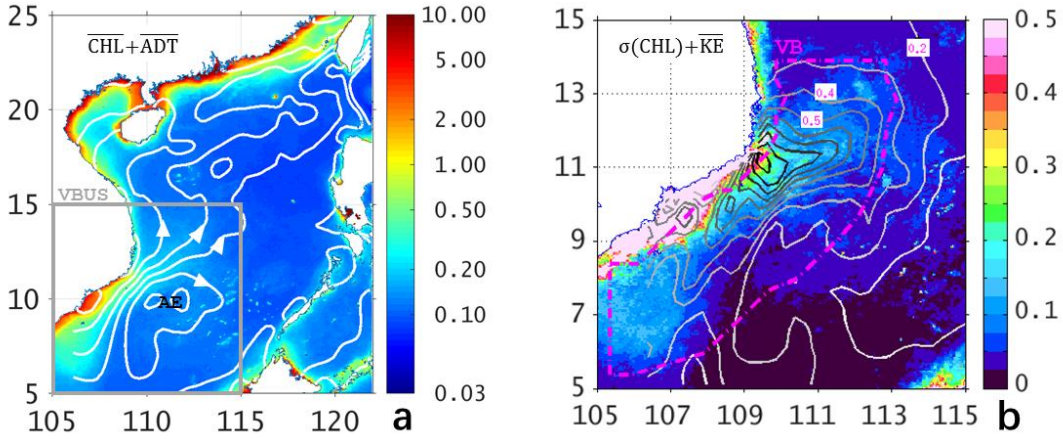

Figure S4 Revised Fig. 2.

References

Gill, A. E.: Atmosphere-ocean dynamics, Academic press, 1982.

Loisel, H., Vantrepotte, V., Ouillon, S., Ngoc, D. D., Herrmann, M., Tran, V., Mériaux, X., Dessailly, D., Jamet, C., Duhaut, T., Nguyen, H. H., and Van Nguyen, T.: Assessment and analysis of the chlorophyll-a concentration variability over the Vietnamese coastal waters from the MERIS ocean color sensor (2002–2012), Remote Sens. Environ., 190, 217-232, 2017.

Oey, L.-Y., Chang, Y.-L., Lin, Y.-C., Chang, M.-C., Varlamov, S., and Miyazawa, Y.: Cross flows in the Taiwan Strait in winter, J. Phys. Oceanogr., 44, 801-817, 2014.

2. Reviewer#2

The authors present a study of the physical-biological coupling of the coastal upwelling off Vietnam. They use in situ, remote sensing and model data. The model is validate with the in situ and remote sensing data, which gave some confident to its outputs. The MS is well written and present interesting results, concluding with a schematic interpretation of the processes related to the variability of primary productivity. Thus, it is my opinion that the MS should be accepted after minor revision taking into the account the comments I made directly in the PDF in annex.

We thank the positive comments and careful editing from the reviewer. Following the comments in the pdf file, we revised the manuscript as listed below.

Separation from what? coast?

Line 21: Yes, separation in the manuscript indicates alongshore current separates from the coast. Modified.

(inventory should be) concentration?

Line 23: We use the depth-integrated nitrate concentration, which is the nutrient inventory here. The unit is mmol m^{-2}.

Indicate these locations in Fig. 1)

Line 27: Figure 1 revised as follows. We added several labels of the geographic locations.

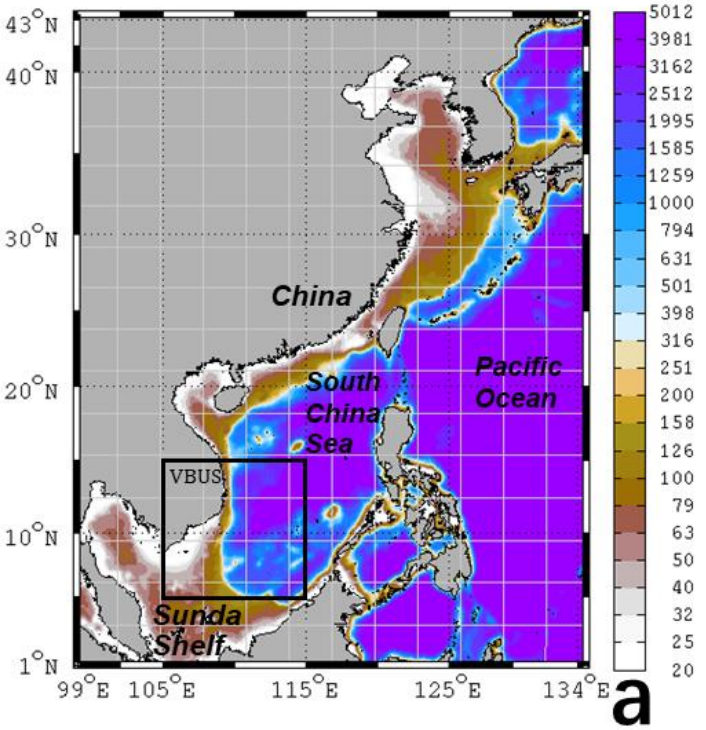

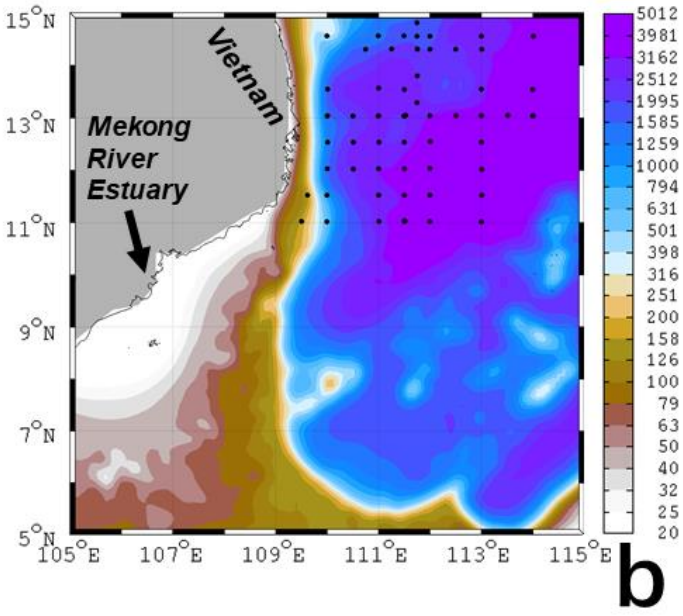

'It is not the best reference. Exampes of more appropriate ones: Cushing (1969). Upwelling and fish production. FAO Fish. Tech. Pap. 84. Bakun (1996). Patternis in the ocean. Cal. Sea Grant'

Line 32: Thank you for providing these references. Cushing (1969) and Bakun (1996) were added to the citation list.

This is the so called "Bakun Index", thus Bakun (1973) is the proper reference.

Line 115: Revised. Now this sentence read: "We use the upwelling intensity (UI) **or the "Bakun index" (Bakun, 1973)** as a proxy to measure the strength of upwelling (Chen et al., 2012; Gruber et al., 2011), following the classical paper of Ekman (1905)…"

the estimated parameters of the regression
(magenta 'box' should be) contour

Line 131&133: Agree and corrected.

In my opinion it also has 2 peaks and even more clear than NPP

Line 213: Agree. This sentence was modified as: "**KE and NPP both present biannually signals in most years**, i.e., peaks in summer and winter, as well as complex non-seasonal signals"

indicate also the p-value

Line 215: here "$p<0.01$" was added.

despite the variability explained

Line 217-224: Notice that we removed this sentence and replaced it with more relevant discussion.

'could be'

Line 294: Corrected as "these shortcomings **could be** accepted."

'other'

Line 315: Corrected.

'presented in'

Line 414: Now it reads: "As **presented in** the schematic diagram in Fig. 12,"

Should be included at the end of the MS, not in supplementary material.

Line 440: We included the abbreviation in appendix A following Sect. 6. We also removed some unnecessary acronyms to increase the readability.

Is this scale the same one for both plots?

'The magenta contour delimit the ocean region over which CHL and KE are averaged.'

'for the region of interest'

Fig. 2: The scales for two subplots were the same. However, noting that in Fig. 2a the nearshore CHL can be as large as 5.0 mg m^{-3} exceeding the color scale, we replaced the color scale with a log2 scale as follows. We also revised the caption following your suggestions. Thank you.

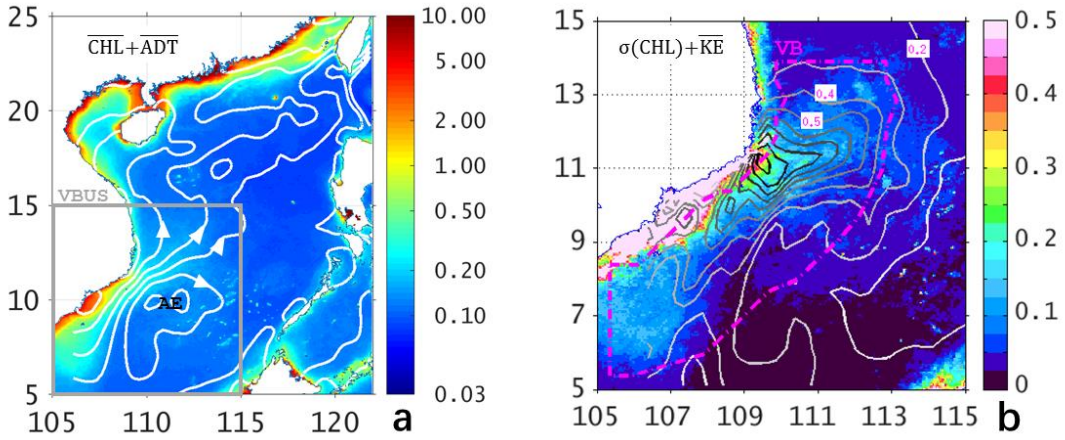

Figure 2 (a) Summertime (MJJAS) average of surface chlorophyll concentration (color shading, unit: mg m^{-3}) from MODIS, overlapped white contours are mean ADT with the arrows showing the directions of geostrophic currents. Gray box is the region of interest (VBUS), while AE shows the center of the anticyclone. (b) **The region of interest:** standard derivation of surface chlorophyll (color shading, unit: mg m^{-3}) overlaid with the contours of surface KE with an interval of 0.1 from 0.1 to 1.0 (unit: m2 s^{-2}). **The magenta dot-dash contour delimits the ocean region over which chlorophyll and KE are averaged (see text)**.

3. Reviewer#3

We thank the reviewer for the comments, which improve our manuscript. Our responses are in blue.

General Comments

1. Most of the scientific papers published about the South China Sea (SCS) are dealing with remote sensing or numerical modeling. Only few papers present in-situ observations, which are ignored by the authors. Unfortunately this is also one of the major problems within this paper, because a couple of relevant papers, which deal with this problem, were ignored. See reference list at the end.

We accept this criticism and have included the additional literature provided by the reviewer and have (briefly) described their relevance to our study in e.g., Line 37, Line 134, Line 171, Line 217, Line 298, and Line 393.

2. The fact that higher wind speed causes a stronger upwelling and a higher nutrient flux into the euphotic zone, which is connected with higher primary production, is not new. It is text book knowledge. This process has been quantified in the SCS upwelling area for normal and post El Nino years inside the upwelling area and offshore (Voss et al. 2006, Bombar et al. 2010). Hence the finding of the authors is not new. It is known since more than 10 years!

(See also related response to Comment#4 below).

In this response, we want to clearly define what is meant by "text book knowledge" of wind-induced upwelling: it is direct wind-induced upwelling in the ("text-book's") sense of "quasi two-dimensionality" of a cross-shore-vertical section coastal ocean upwelling driven by along-shore wind. The definition includes a coast, along-shore wind with scale that is much larger than the baroclinic radius of deformation (i.e. basically spatially uniform wind), and a rotating ocean basin which may have a sloping shelf (e.g. Gill's book, 1982). In the following, this will henceforth be referred to as 'text-book upwelling'.

We agree that the direct wind-induced upwelling and its potential connection with higher primary production is well studied. However, the real world of biophysical inter-connection is (fortunately) far richer than what we might have learnt in 'text books.'

Recent examples of productivity not directly wind-induced (in the text-book's sense) in boundary currents are: Nguyen et al. (2015) and Oey et al. (2018). In these works, it is clear that the text-book upwelling dynamics has little connection with productivity. In the

Vietnam upwelling region, Voss et al. (2006), for example, also noted that the Mekong River may explain the much higher nitrogen fixation outside the upwelling strip of the coast, presumably in part due to increased stratification caused by the spreading of lower surface salinity in the river plume [e.g. Oey and Mellor (1993)]. Voss et al. (2006) did not dynamically demonstrate that increased stratification was the cause, but we tend to agree with them, as we explained dynamically in Huang and Oey (2015) and Lin and Oey (2016). It is clear that currents and dynamics other than the text-book upwelling circulation play a role. Our model in the present study is based on the primitive equation with thermodynamics; 'circulation' here therefore includes also effects of stratification (i.e. baroclinicity). It is not obvious how one might *clearly* separate the different effects, as the strength of the text-book upwelling is most likely linked to other processes.

In our study, we found that, in addition to text-book upwelling, the kinetic energy (KE) of the current and anticyclone (i.e., the "circulation") also influence productivity.

In the manuscript, we show and explain (see Table S1 below) the R^2 between the net integrated primary production (NPP) and (a) the upwelling index UI (i.e. text-book upwelling, related to the along-shore wind stress) and (b) the kinetic energy KE of the circulation; the KE is used as a proxy for the strength of the circulation (referred to as simply "circulation"). Table S1 shows that the UI accounts for 45% of the NPP-variance, while KE accounts for 49%, i.e. the KE can explain as much, and actually slightly more, NPP variance than UI. However, the UI and KE are not independent. The KE is in part wind-forced - while the regression analysis cannot tell us cause and effect, it is reasonable in our case to assume this. Thus UI (through the wind stress) accounts for 32% of the KE variance. It is important to realize that this does *not* mean that the *uniform* alongshore wind stress that causes the text-book upwelling can actually explain 32% of the KE variance. This is because the regional wind stress off Vietnam cannot be separated from the large scale wind stress curl that is crucial to the current separation – i.e. the circulation. In other words, text-book upwelling can *at most* explain 32% of the KE variance, most likely less than 32%.

The simple analysis in Table S1 suggests that (1) text-book upwelling alone is unable to explain the full variability of NPP off Vietnam; (2) circulation plays an important role in contributing to the NPP variability off Vietnam; and (3) a large part of the circulation (at least ~68%) is unexplained by the *uniform* regional wind alone off the Vietnamese coast.

Table S1 R-squared[#] among variables average within VBUS region

X \ Y	NPP	UI	KE
UI	0.4548	-	0.3240
KE	0.4930	0.3240	-
UI & KE	0.6046	-	-

# p<0.01 for all correlations. NPP: Net integrated primary production; UI: Upwelling intensity; KE: Kinetic Energy.

The main goal of our study is to understand and explain the role of the circulation in contributing to the NPP variance. We found, and quantitatively demonstrated using model experiments, that the boundary current separation plays an important role. We therefore agree with the reviewer about the important role of current separation, but fundamentally disagree with the Dippner et al. (2013) interpretations, who as explained below (in Comment 4) mis-applied the Marshall and Tansley (2001) formula.

3. In the abstract the sentence "The elevated kinetic energy and intensified circulation can be explained by the separation of the upwelling system" is the same misinterpretation as in the Liu et al. (2002) paper. The opposite is true. The stronger monsoon intensifies the circulation. If the velocity reach a critical value a jet is detached from the coast.

We agree that this sentence may be misleading. Here we did not attempt to emphasize causality relation. Now the modified sentence reads:

"Results from a physical-biological coupled model reveal that the elevated kinetic energy **is linked to** the strength of the current separation from the coast." (Line 19)

We added the following discussion as Appendix A:
"Qualitatively, both the analysis based on remote sensing data and model results suggest the separation flow is linked with stronger KE (~65% larger in HNA case then LNA case, Sect. 3.1). Moreover, a separation index is defined to quantitatively explain the relation between the flow separation and intensified circulation. The separation index (SI) can be written as:

$$SI = \sum \frac{u \cdot \cos\varphi + v \cdot \sin\varphi}{\sqrt{u^2 + v^2}}, \qquad \text{(S1)}$$

where u and v are the two surface velocity components, and φ is the angle between the topography gradient and the positive x axis. This SI is essentially the area-averaged cross-isobath velocity normalized by the magnitude of the velocity, which is used to quantify flow separation here.

Fig. S1 shows the distribution of SI in Aug 2010. Positive values indicate that the flow is separating and downslope, and that may be seen off Vietnam south of the coastline bend. Large SI (~1.0) can be observed near the separation point ~11.5°N. Taking spatial average over the box region in Fig. S1, there is a good positive correlation (R=0.7175, p<0.01) between log(KE) and SI (see Fig. S2). Moreover, SI may be seen to generally increase with KE to a value of 0.25~0.3 and then it levels off

(i.e. the slope becomes less) – see the red and blue lines in Fig. S2. The log(KE) and SI thus appears to show a logistic-type behavior, in which SI asymptotically approaches some maximum value (in this case ~0.3). This suggest that the strong flow separation and elevated KE are tightly linked. From Fig. S2, the value of KE ≈ 0.1 m^2s^{-2} appears to be a critical value.

Dynamically, the nonlinear advection term in the momentum equation can be written as the vector invariant form [see e.g., Gill (1982)]:

$$\vec{u}\cdot\nabla\vec{u} = (\nabla\times\vec{u})\times\vec{u} + \nabla(\frac{1}{2}|\vec{u}|^2)$$

This decomposition directly links the nonlinear advection term and the gradient of KE (which scales KE over a length scale L). Meanwhile, the nonlinear advection is an important mechanism in driving flow separation [see, for instance, Oey et al. (2014)]. Stronger advection suggests intense cross isobath flow. Therefore, a dynamic linkage between the flow separation and the intensified KE and circulation can also be established, further supporting this argument.

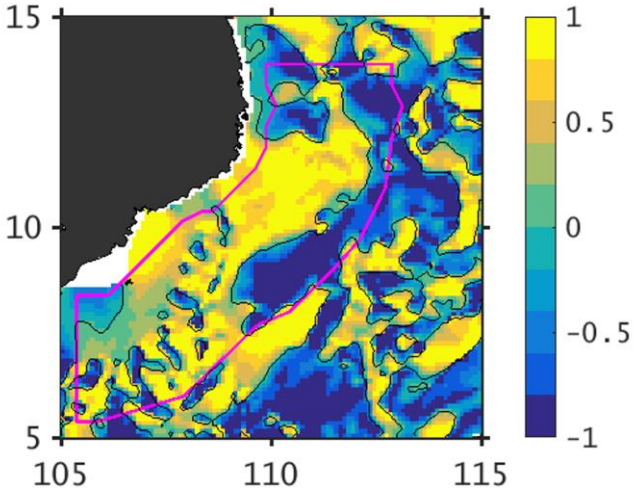

Figure S1 Example of modeled SI in Aug 2010.

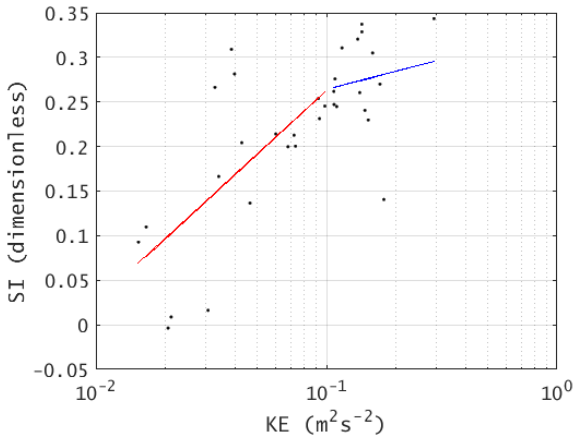

Figure S2 Summer-month (MJJAS) KE vs SI averaged over the box region in Fig. S2 (overall R=0.7175).

(*End of Appendix A)

We respectfully disagree with the reviewer's last 2 sentences: "**The stronger monsoon intensifies the circulation. If the velocity reach a critical value a jet is detached from the coast."** These are based on Dippner et al. (2013). Taken together, and the Reviewer comment#2 above, the reviewer seems to suggest that text-book upwelling intensifies and causes jet separation from the coast. As we point out below, Dippener et al. (2013) mis-applied the Marshall and Tansley (2001) formula.

4. This is the classical Gulf Stream detachment problem discussed by Haidvogel et al. (1992) and Marshall & Tansley (2001). A similar detachment modulated by the ITCZ occurs in the SCS and is described by Dippner et al. (2013). Hence, this aspect is also not new.

Our paper does not deal with western boundary current (WBC) separation, and we checked through the manuscript again to make sure that no such claim is made.

On the other hand, the reviewer's comments are based on the WBC separation issue and the work of Dippner et al. (2013), and there is a need for us to respond.

To the best of our knowledge, the problem of separation of a WBC, the Gulf Stream included, remains unresolved to this date ; the following is from Chassignet and Marshall (2008):

"…Identifying the dynamics responsible for western boundary current separation has been a long-standing challenge. It is fair to say that a proper western boundary current separation … is the result of many contributing factors.. There is yet no single recipe that would guarantee a correct separation …"

Neither Haidvoget et al. (1992) nor Marshall & Tansley (2001) claimed that they solved the WBC separation problem. The authors recognized that the problem is complex and depends on various factors; for examples: wind stress curl, topographic effects including

coastline geometry and bottom topography, inertia & nonlinearity, deep WBC (e.g. the Gulf Stream), unresolved eddies (and how we may parameterize them, as well as the seemingly simple questions of free-slip or no-slip BCs), PV crisis, adverse pressure gradient, boundary current collision, outcropping of isopycnals, multiple equilibria, eddy-topography interaction, surface cooling etc. On reading Dippner et al. (2013), we failed to see how they have dynamically demonstrated the VBUS separation problem. There is a misunderstanding of what a WBC separation is; in particular the authors mis-understood and mis-applied the Marshall and Tansley (2001; MT2001 hereafter) formula (in particular, their equation 11) to the South China Sea.

First, the MT2001 theory is applicable only in steady state, which is not the case of the VBUS forced by the monthly-varying monsoon. In applying the formula, Dippner et al. (2013) therefore implicitly assumed steady state. However, they did not check the validity of this assumption. A lower bound for this time can be estimated based on the time it takes for a long baroclinic wave to propagate across the basin (Anderson and Gill, 1975; Lighthill, 1969), which for SCS is ~ 1,000 km/βR_d^2. The mode-1 baroclinic radius of deformation $R_d \approx 80$ km near the separation latitude (Fig. S3 below). Thus the required time (lower bound) is ~ 90 days. The summertime VBUS WBC is likely to be continually varying and quite unsteady under the monthly varying monsoon wind (Fig. S4 below).

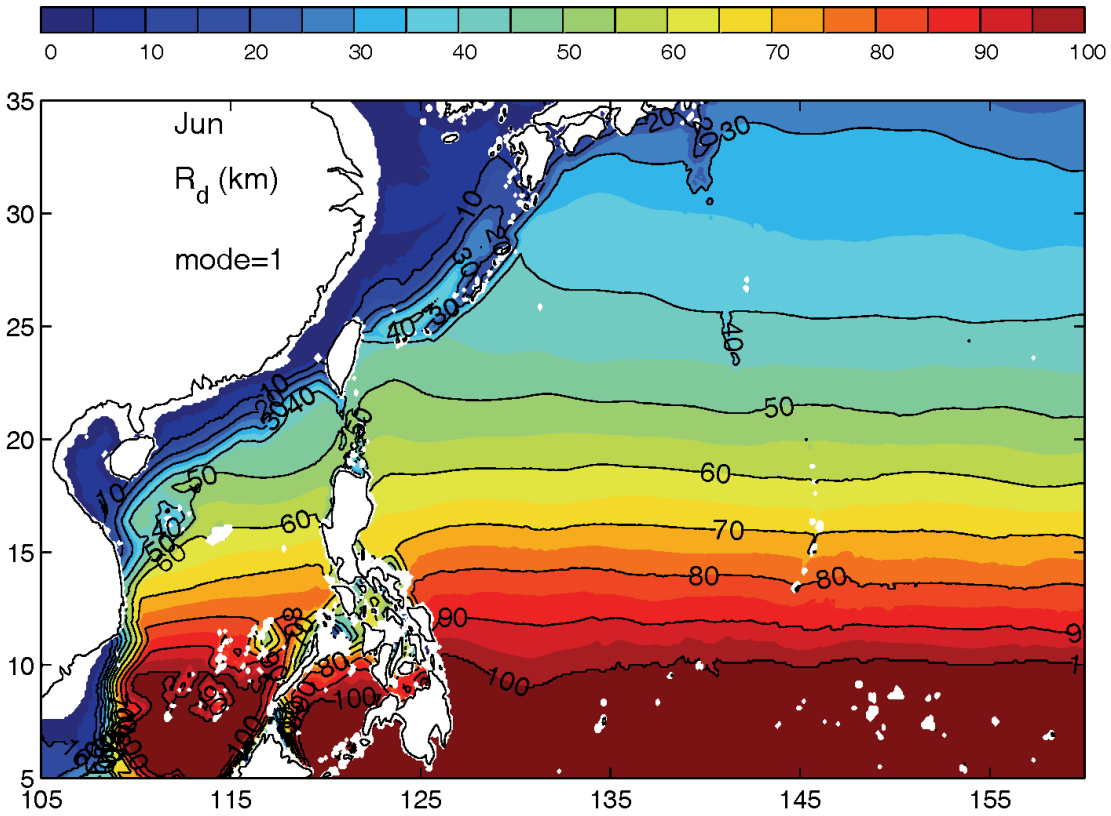

Figure S3 Baroclinic Rossby radius of deformation R_d based on the WOA June climatology [see e.g. (Xu and Oey, 2015)].

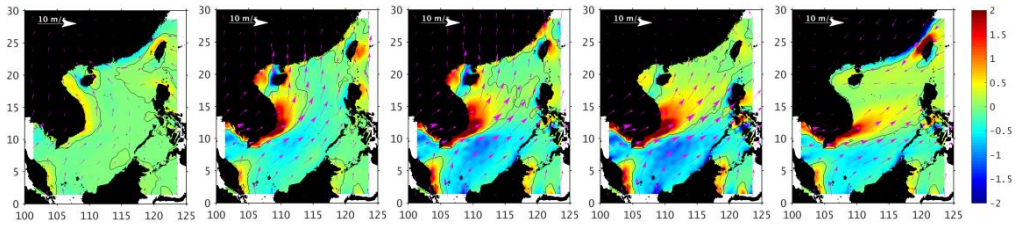

Figure S4 South China Sea monthly climatological wind (m/s; vector scale in top left) and wind stress curl ($\times 10^{-7}$ N/m^3; color shading) based on the CCMP wind data from 1988 to 2009), for the month of (from left to right) May, June, July, August and September (same months as used in Dippner et al. 2013), showing significant monthly variation both in wind and wind stress curl.

Second, even if we assume that quasi-steadiness has been reached, the form of Marshall and Tansley's formula used by Dippner et al. is valid only for a coastline with a vertical wall (no shelf, no slope). This assumption is clearly invalid for Vietnam coast (see Fig. S5 below) characterized with a shelf/slope that narrows to the 'cape' (i.e., separation point), which further more is where/when such a topography convergence favors separation - the middle term of equation 8 in Marshall and Tansley (2001) neglected by Dippner et al.

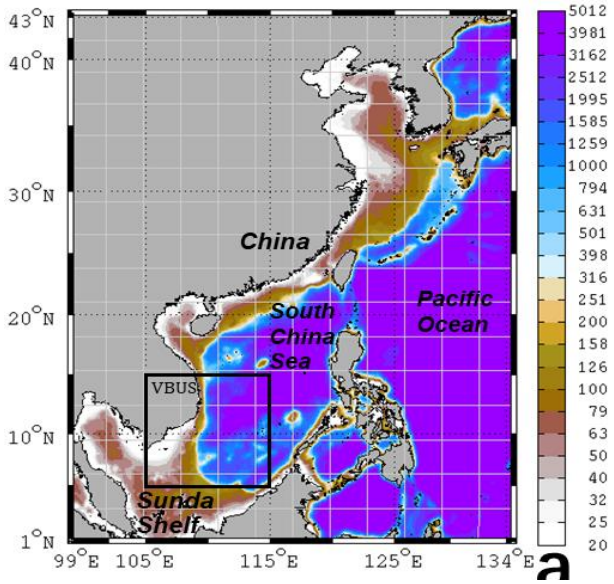

Figure S5 Bottom topography (in meters) of the SCS, from Fig.1a of the manuscript.

Third, let us further relax the assumptions and assume that the vertical-wall coastline is appropriate. For the Gulf Stream, Marshall and Tansley used the 200-m isobath – firstly because it is a good proxy for the path of the Gulf Stream (Figure below), and secondly because their theory is inviscid and is not intended to apply over the shallow shelves, where bottom friction can be strong.

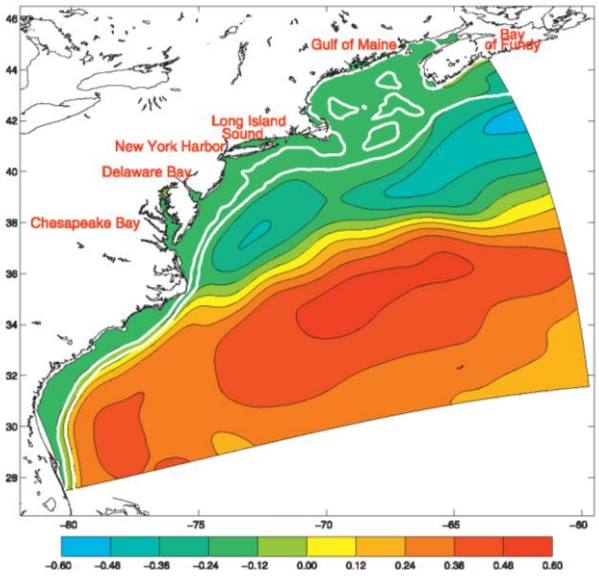

Figure S6 The Gulf Stream region. White contours show the 50 and 200-m isobaths. Color shading and black contours show the 16-year mean (1993-2008) sea-surface height (m) from satellite altimetry (AVISO). Note that the path of the Gulf Stream follows closely the 200-m isobaths up to the separation point where the isobaths makes a sharp turn to the north, as assumed (correctly) by MT2001. [From (Xu and Oey, 2015)].

Using the 200-m isobaths, MT2001 obtained a radius of curvature $r \sim 200$ km. For the SCS/VBUS region (see previous Figure above), the 200-m isobaths runs nearly straight from south to north pass the Vietnamese *coastline* bend near 15°N, yet Dippner et al. used $r = 114$ km – a curvature which is even sharper than that used for the Gulf Stream – which is clearly inappropriate.

These misunderstandings and mis-application of Marshall and Tansley (2001) lead to a false interpretation of the separation dynamics – e.g. Fig.6 of Dippner et al. (2013).

ENSO events & ITCZ analyzed in Dippner et al.:

The authors suggested that in post non-El Nino (i.e. "normal" year) 2004, "…The upwelling and the offshore transport of WM2 and OSW resulted in a blocking of the northward transport of MKGTW and caused the mentioned current separation…" This was contrasted with a post El Nino year 2003 without such 'blocking.' Authors alluded the difference to the intensity of upwelling (which we assume here is the "text-book" type mentioned by the reviewer in Comment#2 above) by the stronger SW monsoon wind in 2004, and then proceeded to apply the Marshall and Tansley (2001) formula (inappropriately as we have already shown above). The ITCZ conclusion was based on this "intensity of upwelling hypothesis" which we now examine.

While we agree that upwelling contributes to increased productivity etc (See response to Comment#2 of the role of 'circulation'), wind-driven upwelling current does not lead to

current separation, no matter its strength. We show this using idealized model experiments to isolate physics.

A South China Sea domain 99-122E & 0-25N is used, closed on all 4 lateral boundaries to ensure a simple zero inflow/outflow boundary condition. In particular the influence of Kuroshio intrusion variability through the Luzon Strait (Chang and Oey, 2012; Lin et al., 2016; Xu and Oey, 2015, 2014) is eliminated to focus on wind-driven responses. The initial temperature is a function of "z" only: $T(z)=2+24*\exp(0.0018*z)$, which approximates the observed climatologically mean vertical profile in South China Sea [see e.g. (Lin et al., 2016)], the salinity is set constant = 35 psu (and remains so through the integration as no rivers nor surface fluxes were specified), and the ocean is at rest. At the surface, all fluxes are nil except the momentum flux i.e. wind stress. A seasonally-varying wind climatology from the long-term CCMP data was used to force the model. For each of the 4 experiments below, the model was integrated for 3 years, and after allowing 2-year spin up for the solution to reach quasi-equilibrium [see Xu and Oey (2015), and references cited therein], the third year output was analyzed. The four experiments are now described.

Exp.NoCurlNoTopo: The basin depth was set constant at 4000 m (i.e. no topographic variation), and the zonal and meridional climatological wind components were averaged meridionally and zonally respectively to eliminate wind curl (i.e. no curl; Figure S7 below, left panel). Thus the coast has a vertical wall and under a summertime southwesterly wind off the southeastern coast of Vietnam (8N~12N), this experiment approximately simulates the 'classical' wind-driven upwelling process (Gill, 1982): offshore surface Ekman transport compensated (approximately in this case) by onshore bottom Ekman transport, and up-lifted isopycnals near the coast where cooler water surfaces, balanced through thermal wind by an along-shore coastal jet that is strongest near the surface. The jet's width is approximately the mode-1 baroclinic radius of deformation $R_d \approx 80$ km (see Figure given previously, or Xu and Oey (2015). The cool surface water shows up as a thin strip of lower SST (< 27.5 ^oC; middle panel) that clings close to the Vietnamese coast, from southeastern coastline around the bend to about 16N latitude. In the 3-D simulation, the coastal jet becomes unstable (Durski and Allen, 2005), as seen in the wavy structure of the 27.5 ^oC isotherm and the meandering current with offshore jets and spun eddies (right panel). Importantly, the sea-surface height SSH is small i.e. the surface is nearly everywhere flat (middle). There is no WBC and obviously one *cannot* apply the Marshall & Tansley formula. Except for the above-mentioned eddying flow from the unstable coastal jet, there is no boundary current separation.

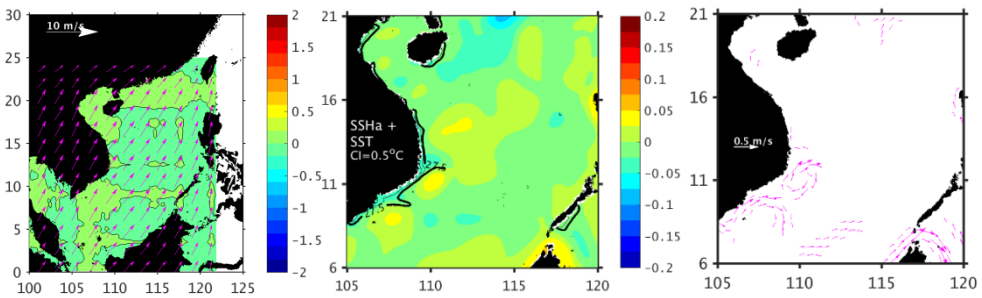

Figure S7 The idealized experiment Exp.NoCurlNoTopo: constant-depth ocean forced by spatially uniform wind without curl. Shown are July mean fields: (left) wind vectors and wind stress curl ($\times 10^{-7}$ Pa/m, color shading); (middle) SSH anomaly (m; color shading) and SST (°C, showing only those <27.5; contours); and (right) surface to 50 m averaged currents (vectors with speeds < 0.1 m/s omitted for clarity).

Exp.NoCurlWithTopo: The model basin now has realistic topography, but the wind is still spatially uniform without curl (Figure below). Over a sloping shelf, a prograde front [frontal and bottom slopes have the same sign, see e.g. (Oey, 2008)] is stabilized by topography (Mysak, 1977). This may be seen in the current plot (right panel) and a comparison with the corresponding flat-bottom case discussed above; off the Vietnamese southeastern coast, the current now flows parallel to the coastline with little meanders. Friction is also increased over the shallow shelf and the water is more vertically mixed near coast; the prograding (upwelling) front is confined to the outer shelf and slope (Allen et al., 1995) and along most of the southeastern coastline south of the bend, the near-coast SST is not as cool as for the flat topography experiment Exp.NoCurlNoTopo, shown previously. As a result, the coolest water now is advected toward and accumulates near the bend, where isobaths rapidly converge. The SSH again shows weak signal south of ~12N, no WBC, and no boundary current separation. [There are eddies in the northern half of the basin due to some kind of dynamical instability (Lin et al., 2016; Oey, 2008; Xu and Oey, 2015) which, while they may be interesting, has little relevance to the separation issue being discussed.]

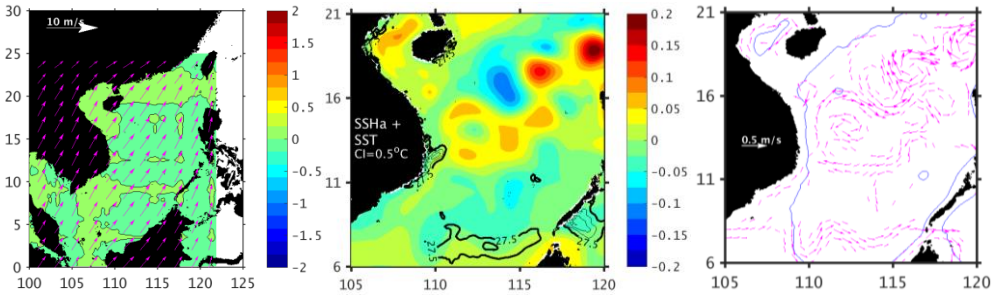

Figure S8 The idealized experiment Exp.NoCurlWithTopo: ocean with realistic topography forced by spatially uniform wind without curl. Shown are July mean fields: (left) wind vectors and wind stress curl ($\times 10^{-7}$ Pa/m, color shading); (middle) SSH anomaly (m; color shading) and SST (°C, showing only those <27.5; contours); and (right) surface to 50 m averaged currents (vectors with speeds < 0.1 m/s omitted for clarity); the blue contour shows the 200-m isobath.

Exp.WithCurlNoTopo: The model now is forced with the spatially non-uniform climatological wind stress but the basin depth is set constant at 4000 m (Figure below). Off Vietnam, the wind stress curl shows a dipolar pattern positive (negative) north (south) of the bend near 12N. The wind stress curl drives southward (northward) Sverdrup interior flow in the southern (northern) South China Sea, and a northward (southward) WBC along the Vietnam's coast (Gill, 1982; Pedlosky, 2013), as can be clearly seen in the current plot (right panel). The SSH also forms a dipole, negative (positive) north (south) near the bend mirroring the wind stress curl dipole, as can be

expected. In the southern half of the basin the SSH is visibly higher compared to the previous NoCurl experiments. Because of the seasonally varying wind forcing, both WBC systems are continually evolving, and are never in a steady state. Nonetheless, boundary current separation can be seen off the bend near 12N, and is clearly forced by the wind stress curl dipole, not by the upwelling current which we already show in Exp.NoCurlNoTopo above produces no such separation. Comparing the SST for the two cases, it is also clear that the offshore ejection of cool water near the bend is strongly controlled by the separation, forced by the wind stress curl dipole.

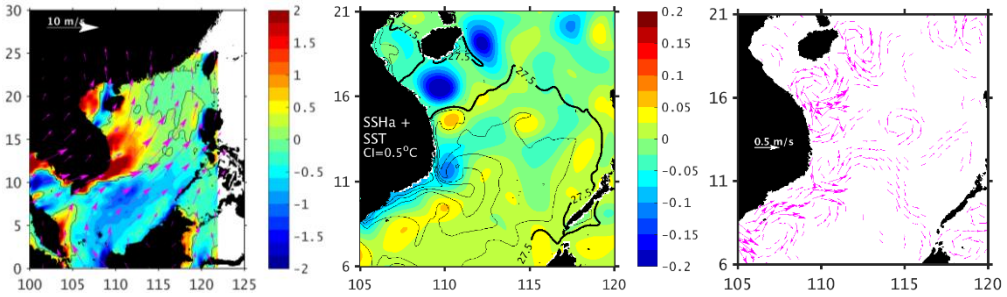

Figure S9 The idealized experiment Exp.WithCurlNoTopo: constant-depth ocean forced by wind with curl. Shown are July mean fields: (left) wind vectors and wind stress curl ($\times 10^{-7}$ Pa/m, color shading); (middle) SSH anomaly (m; color shading) and SST (°C, showing only those <27.5; contours); and (right) surface to 50 m averaged currents (vectors with speeds < 0.1 m/s omitted for clarity).

Exp.WithCurlWithTopo: The final experiment now has realistic topography and is forced by the spatially non-uniform climatological wind stress. With the sloping shelf and slope, the SSH-dipole, hence also the separating current near 12N, become significantly stronger (Figure below). As isopycnals are dynamically lifted near the coast, more cooler subsurface water is brought near the surface along the southeastern coast of Vietnam, and the ejected water in the separated current becomes cooler and more extensive. Note however that, unlike the above constant-depth experiment Exp.WithCurlNoTopo, the northward-flowing WBC off the southeastern Vietnamese coast can no longer be supported by the planetary beta alone. Topographic beta now becomes important due to the northwestward sloping shelf off the southeastern coast of Vietnam. Together with bottom friction, topographic beta now contributes in modifying the WBC, as can be seen by comparing the currents in the two experiments (Csanady, 1978; Xu and Oey, 2011).

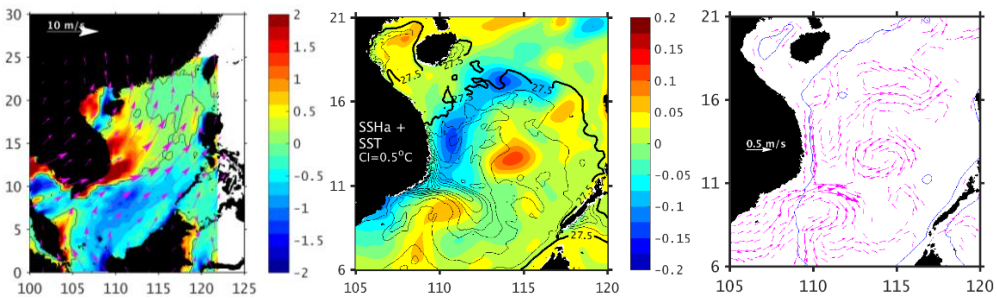

Figure S10 The idealized experiment Exp.WithCurlWithTopo: ocean with realistic topography forced by wind with curl. Shown are July mean fields: (left) wind vectors and wind stress curl ($\times 10^{-7}$ Pa/m, color shading); (middle) SSH anomaly (m; color shading) and SST (^{o}C, showing only those <27.5; contours); and (right) surface to 50 m averaged currents (vectors with speeds < 0.1 m/s omitted for clarity); the blue contour shows the 200-m isobath.

In summary, these experiments clearly demonstrate that the idea that boundary current separation off the Vietnamese coast is caused by the wind-driven upwelling current (Dippner et al. 2013) is incorrect. A WBC cannot be formed by a wind-driven upwelling current, and therefore the application of the Marshall and Tansley's formula to the wind-driven upwelling current cannot be correct. It follows that attempts to explain the current separation and productivity by the strengths of upwelling current – the ENSO variability explained in Dippner et al, cannot be correct. Indeed, our experiments show the importance of the wind stress curl dipole. This suggests that the curl, instead of the intensity, of the wind is major driving factor of the separation. The absent of cold-water during post-ENSO summer is a result of weak wind stress curl (Figure below) and weak separation (compare the above experiments: Exp.WithCurlWithTopo and Exp.NoCurlWithTopo). This explains the co-occurrence of cold water core and current separation in most years, since they are both largely controlled by the wind stress curl.

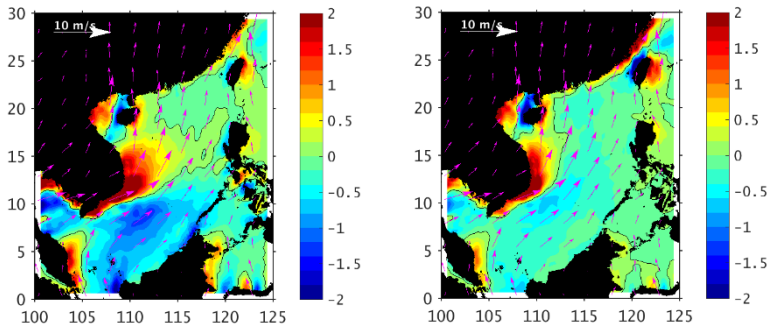

Figure S11 Wind vectors and wind-stress curl during (unit: $\times 10^{7}$ Pa m^{-1}) in Jul of normal years (left) and post-El Nino years (right).

Our linear experiment, presented in the manuscript, also shows a very weak separation, suggesting that intrinsic (nonlinear) dynamics of the ocean is important.

Last but not least, the physical-biological coupling (i.e., how the current modulates the productivity) in the VBUS was also less clear, especially about the quantification and detailed process. This is the main focus and finding of this manuscript, as in the abstract: "Here we show a close spatio-temporal covariability between primary production and **kinetic energy**." "The separated current forms an eastward jet into the interior South China Sea, **and the associated southern recirculation traps nutrient and favors productivity."**

5. The model application is not well posed and the validation is rather problematically. The discussion is a mixture of trivial statements and speculations. These aspects are outlined below. In addition, I have problems with the presentation. There are many Chinese references, however, I miss the fundamental theoretical papers on upwelling (see references) as well as the classical papers on upwelling observations, which are given e.g. in the references of the review by Mittelstaedt (1986).

There are actually no references in the Chinese language in the citation list, we do not want to think you actually meant "the references with Chinese authors". We cited papers which studied this field in this region and every reference was published in major journals in English and is worthy of citing. As you suggests, we added more fundamental theoretical papers in the citation list in e.g., Line 37, Line 134, Line 171, Line 217, Line 298, and Line 393.

6. To conclude: I cannot find any aspect, which merits publication. The paper is a mixture of textbook knowledge, physical misinterpretation, trivial statements, speculation and improper referencing. Therefore, I recommend the editor to reject the paper.

We strongly do not agree with these points. Again, it should be emphasized that the main focus of this study is the current system's influence on the productivity off the Vietnam coasts, instead of the upwelling strength directly from the monsoon wind and its interannual variability. As explained in Comment 2, the variation of the circulation intensity explains additional variability in the production, which cannot be explained by the 'textbook upwelling' alone. Furthermore, although the mechanisms of current separation were already investigated by previous studies, the quantification of its influence on the ecosystem has never been investigated before, and the detailed physical-biological coupling processes are yet unclear. We quantify the recirculation's (and nonlinear effects') role, and provide an underlying mechanism. These are new in this study. To be more specific, we modified the title to "The Modulation of Nonlinear Circulation to the Biological Productivity in the Summer Vietnam Upwelling System".

Specific Comments

7. The motivation of this paper, the so-called "contradictory conclusion", is funny. There is no contradiction. Both papers, the Hein et al. (2013) and the Liu et al. (2002), are correct. The conclusions in these papers were different, because different years were considered. The observations in the Hein paper were made in 2003, whereas the observation in the Liu paper were made in 1992, 1998 and 1999. The authors may have a look to the Multivariate ENSO Index. Drifter observations in 2003 indicated a lateral transport (Dippner et al. 2011) and the physical mechanisms behind the offshore transport and the transport parallel to the coast were explained by

Dippner et al. (2013). So, what is the scientific question of the paper and what are the hypotheses?

Here we used 'contradictory' to indicate apparent contradiction between literatures emphasizing the wind-induced upwelling (Xie et al., 2003) and those highlighted circulation's role (Kuo et al., 2004; Liu et al., 2002). To avoid confusion, this sentence was modified as: "However, the contribution from the recirculation was seldom quantified and compared with that directly from the upwelling, which motivates us to revisit the VBUS ecosystem and its connection with circulation."

An *annual* regression analysis between the summer-averaged NPP and January Multivariate ENSO Index (MEI) following Xie et al. (2003) draws a similar conclusion to our *monthly* analysis in Table S1. About half (R^2=0.49) of the variability in NPP can be explained by the ENSO variability. Considering both MEI and KE concurrently, the R^2 is 0.74, i.e., 25% more variability in NPP is explained. In addition, KE and MEI are mostly independent (R^2 for KE vs. MEI is 0.22). These are consistent with our analysis in Comment 2, demonstrating that the ENSO is not the only player in the NPP variation.

Hence, the scientific question and hypotheses can be seen, as we emphasized, in Line 84: "While the importance of local current system to the VBUS biogeochemical system has been noted in some previous studies (Dippner et al., 2007; Kuo et al., 2004; Liu et al., 2012; Xie et al., 2003), the detailed processes are unclear. To what extent is the ecosystem in VBUS modulated by local circulation? How does the recirculation modulate productivity? How much does the local circulation contribute to production?"

8. The model has a resolution of 1/10 degree. The width of the upwelling are is 42 km. That means that the upwelling area is resolved with less than 4 grid points. Such a resolution of the upwelling area is not sufficient for any conclusions on dynamical processes. Therefore, I recommend to remove the word "upwelling" from the title.

In this manuscript, instead of the fine structure or mechanism of the upwelling, we study the production attributed to the recirculation related to the separation. Therefore, the focus region of this study is not confined to the "actual" upwelling strip of ~40 km wide as indicated by the first baroclinic Rossby radius of deformation (Dippner et al., 2007; Voss et al., 2006), but extending to a broader offshore region of ~3 degree wide (Fig. 2b, magenta contour). This point is now clarified in Line 133.

9. After spin-up, the model runs from 2002 to 2011 and the period 2005 to 2011 was analyzed. The seasonal signal was filtered and from the inter-annual variability composites of high and low chlorophyll were constructed. However, it is not clear how the "normal year", the "no advection" or the "El Niño" were constructed.

In Fig. 11, El Niño year indicates the post-El Niño summer in 2010, while the normal year means other years from 2005 to 2010. No advection is the result from the experiment (Table 1). We added the information in the caption of Fig. 11.

10. The model considers picoplankton, diatoms and coccolithiphorids as functional groups. These functional groups are not representative for the SCS. Dinoflagellates, Phaeocystis spp. and nitrogen fixing bacteria are not considered, although they play a major role in the SCS phytoplankton (Bombar et al. 2011, Doan-Nhu et al 2010, Loick-Wilde et al. 2017).

Other plankton species can be important in the SCS. However, current understanding and observation data are insufficient to build a spatial and temporal simulation of these species. Further development of existing ecosystem model is required to simulate these groups, which is out of the scope of this study. This point was added to Line 170: "Other planktonic groups can be important in the ecosystem of SCS (Bombar et al., 2011; Doan-Nhu et al., 2010; Loick-Wilde et al., 2017). However, to keep the ecosystem model simple and computationally affordable, these groups are not considered in the CoSINE model."

11. No information is given on initial conditions of the biogeochemical model. Without a sensitivity analysis, the statement that the ecosystem model is insensitive to initial conditions is not serious.

As we showed in Line 177: "The initial distribution of nutrients and dissolved organic matter was also interpolated from the WOA climatological data. Small values were analytically assigned to other ecosystem variables since the ecosystem module was **less sensitive** to the initial conditions of these variables". Some studies related with ecosystem modeling (Lu et al., 2015; Wang et al., 2013) was less sensitive to the initial condition (except for nutrients), which are cited here in Line 180.

12. The authors used HNA and LNA as criteria for the construction of composites. This is rather problematic HNA and LNA are not robust variables. NPP is far away from any similarity with observations. Seasonal variability is much higher than inter-annual variability. There is no serious reason to use HNA- and LNA-composites. Strong and weak monsoon would be much better criteria for the construction of composites.

The motivation of this composite map is to examine the different **circulation pattern** when the production is high/low. This makes the choice of HNA and LNA natural. To show the robustness, composite with different thresholds (75%, 70%, and 60%) is also computed, which presents a similar contrast between HNA and LNA. This point was added to Line 229: "Different thresholds (60% and 70%) were also tested and very similar results can be seen."
In terms of NPP simulation, our model indeed shows some discrepancy, as we noted in the manuscript. However, firstly, the relation between wind, circulation and production

can also be found based on model outputs (Line 282-287). Secondly, the contrast between the upwelling region and offshore region was captured. And the discrepancy may also be related to overestimation of retrieved NPP near the coast (Loisel et al., 2017). For both model and remote sensing NPP, seasonal variability is higher than interannual variability. These give us some confidence to further investigate the physical-biological coupling based on the model.

13. The model validation is not convincing. In this context it is important to state that the 3D figures are not helpful. If the authors present an upwelling model, I would like to see a vertical cross section normal to the coast, which should indicate the upwelling of the isopycnals and the poleward undercurrent, which is a quality criterion of upwelling models (O'Brien & Hurlburt 1972).

As noted in the response to Comment 2, the current system's role in the ecosystem is focused. Our consideration is that 3D figure is capable to show the recirculation of ecosystem variables (e.g., nitrate, organic matter) from different perspectives. The maps of plane and section are shown below, which, for instance, clearly show the doming of isopycnals and northward undercurrent to the deep. This figure was included in the supplementary.

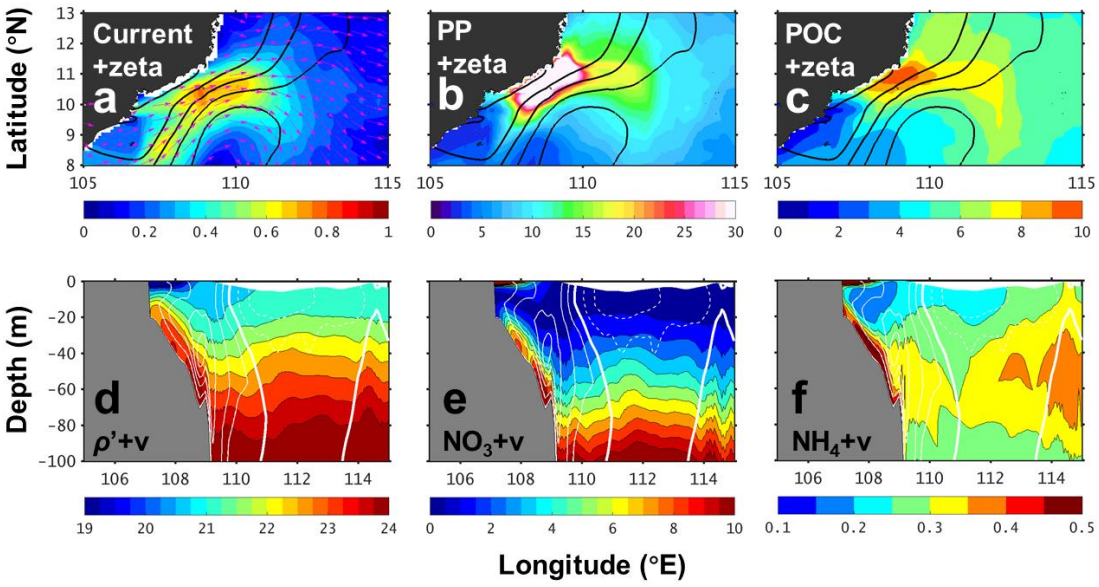

Figure S12 (a-c) Modeled sea level (black contour, CI=0.1 m) overlaid with (a) surface current (color: magnitude in m s^{-1}; vector: flow direction), (b) surface primary production (mg C m^{-3} d^{-1}), and (c) particulate organic carbon (mmol C m^{-3}). (d-f) Sections along 10° N: meridional velocity (positive in solid contours and negative in dashed, CI=0.1 m s^{-1}. Thick contours indicate zero value) overlaid with (d) potential density anomaly, (e) nitrate concentration (mmol m^{-3}), and (f) ammonia concentration (mmol m^{-3}).

14. The model is ~1°C too cold, the modeled NPP does not fit and the estimated kinetic energy is too high. Nevertheless, the authors try to convince the reader on the reasonable well agreement. Furthermore, it should be clearly mentioned that the biannual signals were transient signals, which were not present every year. The authors mentioned that the reasons for discrepancies in validation is insufficient horizontal resolution, unrealistic parameterization etc., but these shortcomings are accepted. Why don't they use a model with a sufficient horizontal resolution, realistic parameterization etc.? Please explain.

We admit that the modeled and observed time-series did not match so well. However, as a process-oriented simulation, the model provides us an approach to investigate the underlying mechanism, considering the focus is to investigate the positive correlation between the productivity and the circulation, which was captured by the model.
We agree that the biannual signal is a transient signal. This sentence was modified as "(appears) in most years…".
The insufficient horizontal resolution is a hypothetical reason. Increasing resolution does not always improve model simulation [see e.g., Sandery and Sakov (2017)]. We hence removed this reason. Notice that all models are simplifications of the real ocean. It is impossible to take all processes into consideration and hence parameters cannot be perfect. Of course, we dream of a model simulation without any bias and if we knew how to further improve the model, we would definitely try our best to improve it.

15. The biogeochemical model produced results far away from reality. From observations, it is known that strong blooms in the upwelling area can be addressed to strong monsoon due to a northern position of ITCZ (Dippner et al. 2013), which causes a specific distribution of characteristic water masses (Dippner & Loick Wilde, 2011) and their corresponding specific species distributions (Loick-Wilde et al. 2017). In contrast, in the oligotrophic offshore area, production can be directly addressed to nitrogen fixing bacteria (Bombar et al. 2010, 2011).

As we emphasized, the focus area of this study is to a broader area offshore ~three-degree wide. The results from Bombar et al. (2010) suggested that the nitrogen fixation "was a significant nitrogen source", which was estimated "2-25% of diffusive nitrate fluxes", but not *all nitrogen source* in the offshore region. Considering the large uncertainty in this estimation, it is very likely that other processes are also playing. And our study showed one possible process, i.e., the nonlinear recirculation related to nutrient trapping, in playing. The conclusion of these paper does not conflict with the papers listed here.

16. L247: The statement "Part of the ammonium could then fuel nitrification and production . . ." is pure speculation. It is not shown.

The *f*-ratio listed in Table 1 was estimated ~0.6, which suggests that that the ammonium supports regeneration production. This point was added to discussion in Line 343.

17. The chapter Discussion has the character of a Results chapter. Normally in the discussion, new findings were discussed in the context of existing literature. This is not done.

Additional discussion associated with existing literatures were added. See the revised part in the manuscript.
E.g., in Line 327: "In the summer VBUS system, it is generally agreed that the wind's predominant role in controlling the variability in the production of VBUS, especially on the inter-annual scale (Dippner et al., 2013). This is also the case in our analysis where UI contributes ~45% of the total variability in production."
Line 333: "The separated current system was considered to transport high-chlorophyll water offshore (Xie et al., 2003). In the offshore region, the production appeared to be elevated (Bombar et al., 2010). However, the fate of the offshore nutrients was rarely investigated in literature."
Line 395 "To a larger scale, the recirculation current couples coastal upwelling and offshore region in major coastal upwelling systems, e.g., in the Canary basin (Pelegrí et al., 2005)."

18. The paragraph on biogeochemical cycles should be skipped. The four mentioned cycles are either trivial or speculation in the sense of not shown. E.g., "upwelled water . . . stimulate high production" is a trivial statement.

We attempt to emphasize that the cycle is important in understanding the recirculation's role in the ecosystem. The four stages of the cycle are supported by analyzing model results. Here we show the evidence one-by-one.
(1) Supported by various papers focus on VBUS [e.g., Dippner et al. (2007)].
(2) Supported by the tongue-like structure of high-chlorophyll water offshore (Fig. 2a and Fig. 9h).
(3) Comparing the high production and low production scenarios in Fig. 10i, where the high production case shows a clear returning flow with high organic matters (Fig. 10h). On the contrary, the low production case presents a tendency of northward transport (Fig. 10g).
(4) The subsurface maxima of ammonium can be seen from Fig. 9f. Bottom Ekman: see high nutrient in the bottom boundary layer in Fig. 9e, and also Gan et al. (2009). The offshore remineralization can be supported by the high oxygen consumption found off Vietnamese coasts (Jiao et al., 2014).
These evidences were added in the text.

19. The paragraph 4.2 is a collection of trivial statements. A comparison of two model runs with and without advection is not helpful in understanding dynamics.

In classical coastal upwelling theory, the role of the nonlinear term is seldom considered. However, in this manuscript, the recirculation related with nonlinear advection appeared to be important. In the derivation of Marshall and Tansley (2001), the nonlinear term is also involved in the governing equation (their equation 1). The experimental case without advection/nonlinear term can be considered as an extreme case where the KE and the separation are very weak with lower production, as we discussed in this section. The nonlinear advection term plays a key role in modulating the ocean circulation, especially in the boundary current systems. So no-advection experiments were designed in many simulation works [e.g. Gruber et al. (2011)].

20. The statement "the more intensive separation, the larger KE in VBUS, and vice versa" in not correct. KE is not a meaningful quantity because separation occurs if the velocity (not KE) reaches a critical value. The statement "high KE is linked to accelerated biogeochemical cycle" is speculation, it is not shown. What means in this context "accelerated". I don't believe that KE has an influence on biological turn-around times.

Additional explanation about the linkage between KE and current separation was added in the Appendix, which shows a critical value of KE can also be used to explain the separation. Actually, considering that KE = $0.5*(u^2+v^2)$, these two arguments are equivalent. Notice that in Table S1 and Comment 2, the KE and separation could be both wind-driven, while KE also presents variability (~68% actually) which cannot directly be explained by the wind speed. We also modified this sentence to "The larger KE, the more intensive separation, and vice versa". (It was "The more intensive separation, the larger KE, and vice versa.")
About the second sentence, the "accelerated" is deleted to avoid the confusion. It is better to put it in: "Low KE reduces the recirculation of nutrients" (corrected in Line 394), which was shown in section 4.2.

21. The conclusion has the character of a summary. It is a repetition of previous speculations.

In the first and second paragraphs of the conclusion, we summarized what was done and what was found in the previous parts of the manuscript. As we show in previous responses, these are supported in our results.
The latter two parts are distinct from the previous ones. In the third paragraph, we illustrate the underlying processes to explain how the recirculation contribute to the production. And in the fourth paragraph, potential research that may be carried out in the future was proposed.

22. The statement "numerical experiment was designed to reproduce the non-separated circulation pattern, while maintaining the external

monsoon forcing" documents not well posed modelling. From literature it is known that the intensity of monsoon and the connected inter-annual variability in ITCZ are responsible for the fine structure in the Vietnamese upwelling area.

Surely the wind's role is very important, but this does not mean that other factors play no role in the separation. Our simulation shows the importance of nonlinear terms, in agree with Wang et al. (2006) and Marshall and Tansley (2001). Also see the discussion in Comment 4. To be more specific, this sentence was revised as "Numerical experiment was also designed to reproduce the **weak**-separated circulation pattern **without the recirculation**, while …"

Technical Comments

23. The ms has too much acronyms.

After removing CHL, POC and NCEP, We found it difficult to further reduce acronyms. We provided a table of all abbreviations in this paper in Appendix A (as Table S2 below).

Table S2 Abbreviations

Acronym	Definition	Acronym	Definition
SCS	South China Sea	NPP	vertical-integrated net primary production
VBUS	Vietnam Boundary Upwelling System	PP	primary production (as a function of depth)
CCMP	Cross-Calibrated Multi-Platform data	KE	kinetic energy
MODIS	Moderate Resolution Imaging Spectroradiometer data	TFOR	Taiwan Strait Nowcast\Forecast system
VGPM	chlorophyll-based Vertically Generalized Production Model	CoSINE	Carbon, Silicon, Nitrogen Ecosystem model
ADT	Absolute Dynamic Topography	NO_ADV	model experiment with no advection term in momentum equations
OISST	Optimum Interpolation Sea Surface Temperature	UI	upwelling intensity
HNA/LNA	high/low-NPP anomaly scenario		

24. The reference Dippner et al. (2006) was published in 2007.

Thanks, corrected.

25. Equation 1 goes back to Ekman (1905), to whom belongs the credit and not Chen et al. (2012) or Gruber et. (2011).

Chen et al. (2012) and Gruber et. (2011) directly applied this equation in studying upwelling. We agree that Ekman (1905) should also be cited here. This index is also known as Bakun Index. Now it goes: "We use the upwelling intensity (UI) or **the "Bakun index" (Bakun, 1973)** as a proxy to measure the strength of upwelling (Chen et al., 2012; Gruber et al., 2011), **following the classical paper of (Ekman (1905))…**"

26. No information on the drag coefficient is given.

Accept. Now the sentence reads: "C_D is the drag coefficient **(constant, 1.3×10^{-3})**".

27. Sloppy formulation: "near-surface geostrophic current". Skip the word geostrophic.

Removed.

28. What is the reference level (layer of no motion) of the dynamic topography? Please explain.

We use absolute dynamic topography (ADT) in this study, which is directly measured by altimetry with respect to the geoid. This point was added in Line 107: "Gridded monthly-mean Absolute Dynamic Topography (ADT) **with respect to the geoid** at 1/4° resolution was acquired."

29. The Statement "nonlinear advection is important to the separation of the coastal jet" should not been addressed to Gan and Qu (2008) or Wand et al. (2006). The credit belongs to Haidvogel et al. (1992) and Marshall & Tansley (2001).

This statement was: "**For the Vietnam boundary upwelling system**, since nonlinear advection is important to the separation of the coastal jet (Gan and Qu, 2008; Wang et al., 2006)". As studies focus on VBUS, Gan and Qu (2008) and Wang et al. (2006) were cited here. We agree that the two classical papers should be cited here. Now it reads: "… is important to the separation of the coastal jet (Gan and Qu, 2008; Wang et al., 2006), **which is familiar in the Gulf Stream separation problem in Haidvogel et al. (1992) and Marshall and Tansley (2001),** …".

30. L165 wrong dimension, should read m^2s^{-2}.

Thank you for your carefulness. Corrected.

31. I cannot see a magenta box.

The magenta dot-dash contour region in Fig. 2b. On the blue background, this color should be clear to see.

32. L202 "the physical and biological parameters" is a wrong formulation. Parameters should be replaced by variable, because a parameter is a quantity, which cannot be measured and must therefore be parameterized, as the name says.

Agree. Modified as "the physical and biological **variables**".

33. L208 Contradiction: Why ageostrophic components contribute to the kinetic energy? This is not compatible with the definition of kinetic energy. Please explain.

Modeled surface velocity includes other components (e.g., from the wind). To avoid misleading, we modified this sentence to "The overestimated KE is partially contributed by the **Ekman** components in the **modeled** surface current."

34. L220 Why a lag suggests a significant regulation of physical forcing? Please explain.

This sentence reads "When NPP is lagged for one month, the correlation is 0.752 with a p-value of 0.0214, suggesting a significant regulation of the physical forcing to the productivity." A p-value of 0.0214 suggests a significant regulation. The lag may be associated with the response time of ecosystem with respect to the physical forcing.

35. L233 What means "the current dissipates freshwater"? Please explain.

This sentence was re-written as: "The current also **disperses** freshwater from the Mekong River,…"

36. The figures are hard to read (too small legends or axes labeling) and not very informative. The main reason is the perspective view, which is surely nice to see, but the essential information remains hidden.

See response to Comment 13. If possible, could you indicate which figure has too small legends or labeling?

References

Allen, J. S., Newberger, P. A., and Federiuk, J.: Upwelling Circulation on the Oregon Continental Shelf. Part I: Response to Idealized Forcing, J. Phys. Oceanogr., 25, 1843-1866, 1995.

Anderson, D. L. and Gill, A.: Spin-up of a stratified ocean, with applications to upwelling, Deep-Sea Res, 22, 583-596, 1975.

Bakun, A.: Coastal upwelling indices, west coast of North America, 1946-71, US Dept. Commerce NOAA Tech. Rep. NMFS-SSRF, 671, 1-103, 1973.

Bombar, D., Dippner, J. W., Doan, H. N., Ngoc, L. N., Liskow, I., Loick-Wilde, N., and Voss, M.: Sources of new nitrogen in the Vietnamese upwelling region of the South China Sea, J. Geophys. Res., 115, 2010.

Bombar, D., Moisander, P. H., Dippner, J. W., Foster, R. A., Voss, M., Karfeld, B., and Zehr, J. P.: Distribution of diazotrophic microorganisms and nifH gene expression in the Mekong River plume during intermonsoon, Marine Ecology Progress Series, 424, 39-52, 2011.

Chang, Y.-L. and Oey, L.-Y.: The Philippines–Taiwan Oscillation: Monsoonlike interannual oscillation of the subtropical–tropical western North Pacific wind system and its impact on the ocean, J. Clim., 25, 1597-1618, 2012.

Chassignet, E. P. and Marshall, D. P.: Gulf Stream separation in numerical ocean models, 177, 39-61, 2008.

Csanady, G.: The arrested topographic wave, J. Phys. Oceanogr., 8, 47-62, 1978.

Dippner, J. W., Bombar, D., Loick-Wilde, N., Voss, M., and Subramaniam, A.: Comment on “Current separation and upwelling over the southeast shelf of Vietnam in the South China Sea” by Chen et al, J. Geophys. Res. Oceans, 118, 1618-1623, 2013.

Dippner, J. W., Nguyen, K. V., Hein, H., Ohde, T., and Loick, N.: Monsoon-induced upwelling off the Vietnamese coast, Ocean Dyn., 57, 46-62, 2007.

Doan-Nhu, H., Lam, N.-N., and Dippner, J. W.: Development of Phaeocystis globosa blooms in the upwelling waters of the South Central coast of Viet Nam, J. Mar. Syst., 83, 253-261, 2010.

Durski, S. M. and Allen, J.: Finite-amplitude evolution of instabilities associated with the coastal upwelling front, J. Phys. Oceanogr., 35, 1606-1628, 2005.

Ekman, V. W.: On the influence of the earth's rotation on ocean-currents, Arkiv. Mat. Astron. Fys., 211, 1-52, 1905.

Gan, J., Cheung, A., Guo, X., and Li, L.: Intensified upwelling over a widened shelf in the northeastern South China Sea, J. Geophys. Res. Oceans, 114, 2009.

Gill, A. E.: Atmosphere-ocean dynamics, Academic press, 1982.

Gruber, N., Lachkar, Z., Frenzel, H., Marchesiello, P., Munnich, M., McWilliams, J. C., Nagai, T., and Plattner, G.-K.: Eddy-induced reduction of biological production in eastern boundary upwelling systems, Nature Geosci, 4, 787-792, 2011.

Huang, S. M. and Oey, L. Y.: Right-side cooling and phytoplankton bloom in the wake of a tropical cyclone, J. Geophys. Res. Oceans, 120, 5735-5748, 2015.

Jiao, N., Zhang, Y., Zhou, K., Li, Q., Dai, M., Liu, J., Guo, J., and Huang, B.: Revisiting the CO2 "source" problem in upwelling areas: a comparative study on eddy upwellings in the South China Sea, Biogeosciences, 11, 2465-2475, 2014.

Kuo, N.-J., Zheng, Q., and Ho, C.-R.: Response of Vietnam coastal upwelling to the 1997–1998 ENSO event observed by multisensor data, Remote Sens. Environ., 89, 106-115, 2004.

Lighthill, M. J.: Dynamic response of the Indian Ocean to onset of the southwest monsoon, Phil. Trans. R. Soc. Lond. A, 265, 45-92, 1969.

Lin, Y.-C., Oey, L.-Y., Wang, J., and Liu, K.-K.: Rossby Waves and Eddies Observed at a Temperature Mooring in Northern South China Sea, J. Phys. Oceanogr., 46, 517-535, 2016.

Lin, Y. C. and Oey, L. Y.: Rainfall-enhanced blooming in typhoon wakes, Scientific reports, 6, 31310, 2016.

Liu, K.-K., Chao, S. Y., Shaw, P. T., Gong, G. C., Chen, C. C., and Tang, T. Y.: Monsoon-forced chlorophyll distribution and primary production in the South China Sea: observations and a numerical study, Deep-Sea Res. Part I-Oceanogr. Res. Pap., 49, 1387-1412, 2002.

Loick-Wilde, N., Bombar, D., Doan, H. N., Nguyen, L. N., Nguyen-Thi, A. M., Voss, M., and Dippner, J. W.: Microplankton biomass and diversity in the Vietnamese upwelling area during SW monsoon under normal conditions and after an ENSO event, Prog. Oceanogr., 153, 1-15, 2017.

Loisel, H., Vantrepotte, V., Ouillon, S., Ngoc, D. D., Herrmann, M., Tran, V., Mériaux, X., Dessailly, D., Jamet, C., Duhaut, T., Nguyen, H. H., and Van Nguyen, T.: Assessment and analysis of the chlorophyll-a concentration variability over the Vietnamese coastal waters from the MERIS ocean color sensor (2002–2012), Remote Sens. Environ., 190, 217-232, 2017.

Lu, W., Yan, X.-H., and Jiang, Y.: Winter bloom and associated upwelling northwest of the Luzon Island: A coupled physical-biological modeling approach, J. Geophys. Res. Oceans, 120, 533-546, 2015.

Marshall, D. P. and Tansley, C. E.: An Implicit Formula for Boundary Current Separation, J. Phys. Oceanogr., 31, 1633-1638, 2001.

Mysak, L. A.: On the Stability of the California Undercurrent off Vancouver Island, J. Phys. Oceanogr., 7, 904-917, 1977.

Nguyen, H. M., Rountrey, A. N., Meeuwig, J. J., Coulson, P. G., Feng, M., Newman, S. J., Waite, A. M., Wakefield, C. B., and Meekan, M. G.: Growth of a deep-water, predatory fish is influenced by the productivity of a boundary current system, Scientific reports, 5, 9044, 2015.

Oey, L.-Y.: Loop Current and Deep Eddies, J. Phys. Oceanogr., 38, 1426-1449, 2008.

Oey, L.-Y., Chang, Y.-L., Lin, Y.-C., Chang, M.-C., Varlamov, S., and Miyazawa, Y.: Cross flows in the Taiwan Strait in winter, J. Phys. Oceanogr., 44, 801-817, 2014.

Oey, L.-Y. and Mellor, G.: Subtidal variability of estuarine outflow, plume, and coastal current: A model study, J. Phys. Oceanogr., 23, 164-171, 1993.

Oey, L.-Y., Wang, J., and Lee, M.-A.: Fish catch is related to the fluctuations of a Western Boundary Current, J. Phys. Oceanogr., 48, 705-721, 2018.

Pedlosky, J.: Geophysical fluid dynamics, Springer Science & Business Media, 2013.

Pelegrí, J. L., Arístegui, J., Cana, L., González-Dávila, M., Hernández-Guerra, A., Hernández-León, S., Marrero-Díaz, A., Montero, M. F., Sangrà, P., and Santana-Casiano, M.: Coupling between the open ocean and the coastal upwelling region off northwest Africa: water recirculation and offshore pumping of organic matter, J. Mar. Syst., 54, 3-37, 2005.

Sandery, P. A. and Sakov, P.: Ocean forecasting of mesoscale features can deteriorate by increasing model resolution towards the submesoscale, Nat Commun, 8, 1566, 2017.

Voss, M., Bombar, D., Loick, N., and Dippner, J. W.: Riverine influence on nitrogen fixation in the upwelling region off Vietnam, South China Sea, Geophys. Res. Lett., 33, 2006.

Wang, J., Hong, H., Jiang, Y., Chai, F., and Yan, X.-H.: Summer nitrogenous nutrient transport and its fate in the Taiwan Strait: A coupled physical-biological modeling approach, J. Geophys. Res. Oceans, 118, 4184-4200, 2013.

Xie, S. P., Xie, Q., Wang, D., and Liu, W. T.: Summer upwelling in the South China Sea and its role in regional climate variations, J. Geophys. Res. Oceans, 108, 2003.

Xu, F.-H. and Oey, L.-Y.: The origin of along-shelf pressure gradient in the Middle Atlantic Bight, J. Phys. Oceanogr., 41, 1720-1740, 2011.

Xu, F.-H. and Oey, L.-Y.: Seasonal SSH variability of the Northern South China Sea, J. Phys. Oceanogr., doi: 10.1175/JPO-D-14-0193.1, 2015. 2015.

Xu, F.-H. and Oey, L.-Y.: State analysis using the Local Ensemble Transform Kalman Filter (LETKF) and the three-layer circulation structure of the Luzon Strait and the South China Sea, Ocean Dyn., 64, 905-923, 2014.

4. Revised manuscript with tracking changes

Starting from next page, the manuscript with tracking changes is shown with new page numbers and line numbers.

~~Physical~~The Modulation of Nonlinear Circulation to the Biological Productivity in the Summer Vietnam Upwelling System

Wenfang Lu[1,2,3,4], Enhui Liao[2,3,4,6], Xiao-Hai Yan[3,4], Lie-Yauw Oey[5,6], Wei Zhuang[2,4], Yuwu Jiang[2,4]

[1]Key Laboratory of Spatial Data Mining and Information Sharing of Ministry of Education, & National Engineering Research Centre of Geo-spatial Information Technology, Fuzhou University, Fuzhou, 350116, China
[2]State Key Laboratory of Marine Environmental Science, College of Ocean and Earth Sciences, Xiamen University, Xiamen, 361102, China
[3]Center for Remote Sensing, College of Earth, Ocean and Environment, University of Delaware, Newark, DE, USA
[4]Joint Institute for Coastal Research and Management, University of Delaware/Xiamen University, USA/China
[5]National Central University, Jhongli City, Taoyuan County, Taiwan
[6]Princeton University, Princeton, New Jersey, USA

Correspondence to: Yuwu Jiang (ywjiang@xmu.edu.cn)

Abstract. Biological productivity in the summer Vietnam boundary upwelling system in the western South China Sea, as in many coastal upwelling systems, is strongly modulated by wind. However, the role of ocean circulation and mesoscale eddies has not been elucidated. Here we show a close ~~spatio-temporal~~spatiotemporal covariability between primary production and kinetic energy. High productivity is associated with high kinetic energy, which accounts for ~15% of the production variability. Results from a physical-biological coupled model reveal that the elevated kinetic energy ~~and intensified circulation can be explained by~~is linked to the ~~separation~~strength of the ~~upwelling~~ current ~~system~~separation from the coast. The separated current forms an eastward jet into the interior South China Sea, and the associated southern ~~gyre~~recirculation traps nutrient and favors productivity. When separation is absent, the model shows weakened circulation and eddy activity, with ~21% less nitrate inventory and ~16% weaker primary productivity.

1 Introduction

The South China Sea (SCS) is a large semi-enclosed marginal sea located in the western Pacific Ocean (Fig. 1a). It is bordered by extensive continental shelves along the southern coast of China and northeastern Vietnam, and the Sunda Shelf south of Vietnam (Fig.1). It has a deep interior basin which can be as deep as 5000 m ~~(Liu et al., 2010; Wong et al., 2007)~~(Liu et al., 2010; Wong et al., 2007). The SCS is predominantly controlled by the East Asian Monsoon. The wind is southwesterly from June to September, and northeasterly from November to March ~~(Liu et al., 2002)~~(Liu et al., 2002). Because of efficient biological production, the interior SCS has a low nutrient concentration in the euphotic zone, displaying ~~a~~an oligotrophic condition (Wong et al., 2007).

~~Coastal upwelling is one of the most important processes for ocean productivity and fishery (Gruber et al., 2011). During southwesterly monsoon, upwelling favorable wind prevails along the southern coast of Vietnam over the complex topography (~~Coastal upwelling is one of the most important processes for ocean productivity and fishery (Bakun, 1996; Cushing, 1969; Mittelstaedt, 1986). During southwesterly monsoon, upwelling-favorable wind prevails along the southern coast of Vietnam over the complex topography (Fig. 1b). The offshore Ekman transport drives surface divergence~~,~~ and results in coastal upwelling of cold and nutrient-rich subsurface water. We refer to this region of interest as the Vietnam Boundary Upwelling System (VBUS). The VBUS is centered near ~109° E between 14° N and 17° N along the coast ~~(Loisel et al., 2017)~~(Loisel et al., 2017)~~. Upwelling in VBUS was confirmed by cruise (Dippner et al., 2006) and remote sensing observations~~. Upwelling in VBUS was confirmed by cruise (Dippner et al., 2007) and remote sensing observations ~~(Kuo et al., 2000)~~(Kuo et al., 2000).

In VBUS, the upwelling intensity is governed by the strength of the alongshore monsoon wind, as in other coastal upwelling systems such as the coastal upwelling systems of California and mid-Atlantic Bight ~~(Gruber et al., 2011)~~(Gruber et al., 2011). The VBUS upwelling strength is intense, and can result in surface cooling of 3~5 °C and an associated cold filament length of ~500 km ~~(Kuo et al., 2004)~~(Kuo et al., 2004). The VBUS is modulated by different climatic variations, such as the El Niño and Southern Oscillation ~~(Dippner et al., 2006; Hein et al., 2013; Xie et al., 2003)~~(Dippner et al., 2007; Hein et al., 2013; Xie et al., 2003)~~, the Indian Ocean Dipole (Liu et al., 2012; Xie et al., 2009), and the Madden-Julian Oscillation (Isoguchi and Kawamura, 2006; Liu et al., 2012).~~

~~The ~~, the Indian Ocean Dipole (Liu et al., 2012; Xie et al., 2009), and the Madden-Julian Oscillation (Isoguchi and Kawamura, 2006; Liu et al., 2012).

Previous studies suggested that both the wind-induced upwelling and the local circulation could influence the nutrient balance and ecosystem in the VBUS ~~are controlled by the ~~. The El Niño variability ~~which modulates~~is an important controlling factor of the VBUS by modulating the summer monsoon ~~(Chai et al., 2009; Kuo and Ho, 2004)~~(Chai et al., 2009; Kuo and Ho, 2004). During post-El Niño summer, the weakened southwesterly wind ~~weakens the~~leads to weak upwelling and ~~reduces the~~reduced upward nutrient flux ~~(Xie et al., 2003)~~(Xie et al., 2003)~~. In addition, Hein et al. (2013) proposed instead that productivity is controlled by lateral transport of nitrate in the VBUS. Liu et al. (2002) also highlighted the role of coastal jet located to south of Vietnam coast. They mentioned that jet induced upwelling was responsible for the nutrient influx. These contradictory conclusions in previous works motivate us to examine the VBUS ecosystem and its connection with circulation.~~

~~Early hydrodynamic observations revealed a northeastward coastal current over the southern shelf of Vietnam (Wyrtki, 1961). The current separates and flows offshore at about 11°N (Xu et al., 1982). Xie et al. (2003) ascribed the jet separation to the strong wind jet off Vietnam due to orographic steering of the north-south running mountains. Using an idealized reduced gravity model, Wang et al. (2006) highlighted vorticity input by wind stress curl and vorticity advection by the basin circulation. Gan and Qu (2008) found that the separation was associated with an adverse pressure gradient induced by the topographic effects.~~

. In addition, Hein et al. (2013) proposed instead that productivity was controlled by lateral transport of nitrate in the VBUS. Liu et al. (2002) also highlighted the role of coastal jet located to the south of Vietnam coast. They mentioned that jet-induced upwelling was responsible for the nutrient influx. Xie et al. (2003) mentioned the role of the offshore jet and resultant quasi-stationary eddy (i.e., the "recirculation" hereafter) in transporting the highly productive water. However, the contribution from recirculation has not been directly quantified and compared with that directly from the upwelling, which motivates us to revisit the VBUS ecosystem and its connection with circulation.

Early hydrodynamic observations revealed a northeastward coastal current over the southern shelf of Vietnam (Wyrtki, 1961). The current separates from the coast and flows offshore at about 11°N (Xu et al., 1982). Xie et al. (2003) ascribed the jet separation to the strong wind jet off Vietnam due to the orographic steering of the north-south running mountains. Using an idealized reduced gravity model, Wang et al. (2006) highlighted vorticity input by wind-stress curl and vorticity advection by the basin circulation. Gan and Qu (2008) found that the separation was associated with an adverse pressure gradient induced by the topographic effects.

The separated jet produces cooling and results in biannual SST variation in the SCS ~~(Xie et al., 2003)~~(Xie et al., 2003). The offshore jet also appears to advect water with high chlorophyll ~~(CHL)~~ to the interior of the central SCS ~~(Chen et al., 2014; Loisel et al., 2017; Tang et al., 2004)~~(Chen et al., 2014; Loisel et al., 2017; Tang et al., 2004). While the importance of ~~circulation~~the local current system to the VBUS biogeochemical- system has been noted in some previous studies ~~(Dippner et al., 2006; Kuo et al., 2004; Liu et al., 2012; Xie et al., 2003)~~(Dippner et al., 2007; Kuo et al., 2004; Liu et al., 2012; Xie et al., 2003), the detailed processes are unclear. To what extent is the ecosystem in VBUS modulated by local circulation? How does the ~~coastal jet~~recirculation modulate productivity? How much does the local circulation contribute to production? Studying biological production and its coupling with physical processes in the VBUS will help to answer these questions and further improve the understanding of boundary upwelling system. Such a study will also shed light on the ecosystem ~~dynamic~~dynamics in the SCS as an oligotrophic marginal sea. Here we analyze the complex dynamics of the VBUS using a physical-biological coupled numerical model system, as well as remote sensing data and *in situ* observations.

This paper is organized as follows. In Sect. 2, the model configuration, numerical experiments, observed data, and statistical method used in this study are described. In Sect. 3, we analyze the remote sensing data and validate the model. Model results from both the standard run and the sensitivity experiment are presented. In Sect. 4, the dynamical processes are analyzed. Conclusions are given in Sect. 5.

2 Model, Data and Methods

2.1 Data

The surface wind vectors were from the Cross-Calibrated Multi-Platform (CCMP) gridded data. This is a 25-year, six-hourly, 1/4°×1/4° resolution product fused from several microwave radiometers and scatterometers using a variational analysis method (Atlas et al., 2011). Monthly Moderate Resolution Imaging Spectroradiometer (MODIS) Aqua level-3 ~~CHL~~chlorophyll (4 km resolution) was obtained from the NASA Distributed Active Archive Center. The estimated monthly vertical-integrated net primary production (NPP) was derived from MODIS ~~CHL~~chlorophyll data via the standard chlorophyll-based Vertically Generalized Production Model (VGPM) algorithm ~~(Behrenfeld and Falkowski, 1997~~(Behrenfeld and Falkowski, 1997)). The VGPM NPP product had a resolution of 1/10 degree, covering the period from 2004 to present. Gridded monthly-mean Absolute Dynamic Topography (ADT) with respect to the geoid at 1/4° resolution was acquired. The 1/4° Optimum Interpolation Sea Surface Temperature (OISST, also known as Reynolds 0.25v2) was constructed by combining the Advanced Very High Resolution Radiometer satellite and other observation data (Banzon et al., 2016). *In situ* observed nitrate and ~~CHL~~chlorophyll profiles from the western SCS stations (Fig. 1b) were used, as detailed in ~~Jiao et al. (2014)~~Jiao et al. (2014).

2.2 Methods

2.2.1 Upwelling Intensity (UI) and Kinetic Energy (KE)

~~We use the upwelling intensity (UI) as a proxy to measure the strength of upwelling (Chen et al., 2012; Gruber et al., 2011):~~

We use the upwelling intensity (UI) or the "Bakun index" (Bakun, 1973) as a proxy to measure the strength of upwelling (Chen et al., 2012; Gruber et al., 2011), following the classical paper of Ekman (1905):

$$\mathbf{UI} = \frac{\tau_y}{\rho_0 f} = \frac{\rho_a C_D U_y |U_y|}{\rho_0 f}. \quad (1)$$

Here, τ_y is the along-shore component of wind stress, f is the Coriolis parameter, ρ_0 is ~~sea water~~seawater density (constant, 1025 kg m^{-3}), ρ_a is the air density (constant, 1.2 kg m^{-3}), C_D is the drag coefficient (constant, 1.3×10^{-3}) and U_y is the alongshore wind speed. The CCMP data with full temporal and spatial coverage close to the coastline is used for the wind speed.

The kinetic energy (KE) of the near-surface geostrophic current is used as an indicator of the circulation intensity. The near-surface ~~geostrophic~~ current is calculated from absolute dynamic topography (ADT) using the geostrophic balance. The KE then equals:

$$\mathrm{KE} = \frac{1}{2}\left(u_g^2 + v_g^2\right) = \frac{1}{2\rho_0^2 f^2}\left[\left(\frac{\partial \mathrm{ADT}}{\partial x}\right)^2 + \left(\frac{\partial \mathrm{ADT}}{\partial y}\right)^2\right], \quad (2)$$

2.2.2 Multivariable Linear Regression

Monthly net primary production (NPP) from VGPM (Vertically Generalized Production Model; see Sect. 2.1 Data) was used to estimate biological productivity. A multivariable linear regression analysis was conducted to examine the statistical relations among NPP, UI, and KE:

$$NPP = b_1\, UI + b_2\, KE + b_3, \quad (3)$$

where b_1, b_2, and b_3 are the estimated parameters of the regression. Data in the summer months (MJJAS) were used since the monsoon wind during this period is upwelling-favorable. ~~We averaged NPP and KE over the ocean region enclosed by the magenta 'box'~~The focus region of this study is not confined to the "actual" upwelling strip of ~40 km wide as indicated by the first baroclinic Rossby radius of deformation (Dippner et al., 2007; Voss et al., 2006), but extending to a broader offshore region of ~three-degree wide. Therefore, we averaged NPP and KE over the ocean region enclosed by the magenta contour off the coast of Vietnam (Fig. 2b). Only the summertime data in the overlapping period from 2004 to 2012 were analyzed. Contributions from SST, day length, and the photosynthetically active radiation were implicitly considered in the VGPM ~~(Behrenfeld and Falkowski, 1997)~~(Behrenfeld and Falkowski, 1997).

2.3 Model Description

We use a three-dimensional general circulation model based on the Regional Ocean Model System (ROMS). ROMS is a free-surface and hydrostatic ocean model. It solves the Reynolds-averaged Navier-Stokes equations on terrain-following coordinates ~~(Shchepetkin and McWilliams, 2005)~~(Shchepetkin and McWilliams, 2005). The model is used in the operational Taiwan Strait Nowcast\Forecast system (TFOR), which successfully provides multi-purpose ocean forecasts ~~(Jiang et al., 2011; Liao et al., 2013; Lin et al., 2016; Lu et al., 2017; Lu et al., 2015; Wang et al., 2013)~~(Jiang et al., 2011; Liao et al., 2013; Lin et al., 2016; Lu et al., 2017; Lu et al., 2015; Wang et al., 2013). In this study, the model grid is modified to cover the whole SCS domain and part of the North-Western Pacific with a grid resolution of 1/10 degree (Fig. 1a). The number of grid nodes in x- and y-direction are 382 and 500, respectively. In the vertical, 25 σ-levels is used with a grid size of ~2 m on average near the surface to resolve the surface boundary layer. Following the bulk formulation scheme ~~(Liu et al., 1979)~~(Liu et al., 1979), daily atmospheric fluxes are applied at the surface. The atmospheric forcing includes downward shortwave radiation, downward longwave radiation, air temperature, air pressure, precipitation rate and relative humidity, acquired from the National Centers for Environmental Prediction ~~(NCEP)~~ Reanalysis data (http://www.esrl.noaa.gov/psd/data/gridded/data.ncep.reanalysis.html, ~~Kalnay et al., 1996)~~(Kalnay et al., 1996)

distributed by the NOAA/OAR/ESRL PSD, Boulder, Colorado, USA (http://www.esrl.noaa.gov/psd/). The wind vectors are from the CCMP wind. The vertical turbulent mixing uses a K-profile parameterization (KPP) scheme ~~(Large et al., 1994)~~(Large et al., 1994) which was successfully applied in a one-dimensional vertical mixing model in the SCS ~~(Lu et al., 2017)~~(Lu et al., 2017). The KPP scheme estimates eddy viscosity within the boundary layer as the production of the boundary layer depth, a turbulent velocity scale, and a dimensionless third-order polynomial shape function. Beyond the surface boundary layer, KPP scheme includes vertical mixing collectively contributed by shear mixing, double diffusive process and internal waves. Biharmonic horizontal mixing scheme ~~(Griffies and Hallberg, 2000)~~(Griffies and Hallberg, 2000) with a reference viscosity of 2.7×10^{10} m^4 s^{-1} is applied, following the value of ~~Bryan et al. (2007)~~Bryan et al. (2007) used in a circulation model with the same horizontal resolution. Climatological river discharges from the Mekong River and other major rivers are included as point sources.

The biogeochemical module is the Carbon, Silicon, Nitrogen Ecosystem (CoSINE) model ~~(Xiu and Chai, 2014)~~(Xiu and Chai, 2014), which consists of 31 state variables, including four nutrients [nitrate (NO_3), ammonium (NH_4), silicate, and phosphate], three phytoplankton functional groups (representing picoplankton, diatoms and coccolithophorids), two zooplankton classes (i.e., microzooplankton and mesozooplankton), four detritus pools (particulate organic nitrogen/carbon, particulate inorganic carbon, and biogenic silica), four dissolved organic matters (labile and semi-labile pools for both carbon and nitrate), and bacteria. Other planktonic groups can be important in the ecosystem of SCS (Bombar et al., 2011; Doan-Nhu et al., 2010; Loick-Wilde et al., 2017). However, to keep the ecosystem model simple and computationally affordable, these groups are not considered in the CoSINE model. The CoSINE model was successfully applied in the study on the primary production ~~(Liu and Chai, 2009)~~(Liu and Chai, 2009), mesoscale eddy and its impacts ~~(Guo et al., 2015)~~(Guo et al., 2015), and the phytoplankton community structure ~~(Ma et al., 2013, 2014)~~(Ma et al., 2013, 2014) in the SCS.

The physical modeled was initialized from a resting state with temperature and salinity specified using the World Ocean Atlas (WOA2013, https://www.nodc.noaa.gov/OC5/woa13/) climatology. The initial distribution of the nutrients and dissolved organic matter was also interpolated from the WOA climatological data. Small values were analytically assigned to other ecosystem variables since the ecosystem module was ~~insensitive to the initial conditions, except for nutrients.~~less sensitive to the initial conditions of these variables (Lu et al., 2015; Wang et al., 2013). After spinning up for 13 years with climatological forcing, the model was restarted with the ecosystem module driven by interannually-varying CCMP wind and ~~NCEP~~atmospheric surface forcing from 2002 to 2011. The model outputs from 2005 to 2011 are analyzed.

2.4 Sensitivity Experiment

~~To quantify the contribution to ecosystem from coastal jet, we seek to control the coastal jet separation while maintaining the larger basin-scale circulation. For the Vietnam boundary upwelling system, since nonlinear advection is important to the separation of the coastal jet (Gan and Qu, 2008; Wang et al., 2006), an experiment without the nonlinear advection terms in the momentum equations was conducted (e.g. Gruber et al. 2011). We note~~

~~that the advection terms in the tracer equations are retained for transport of active and passive tracers (i.e., ecosystem variables). Hereafter, this experiment will be referred as NO_ADV run.~~

To quantify the contribution to the ecosystem from the recirculation, we seek to control the formation of the recirculation while maintaining the larger basin-scale circulation. For the Vietnam boundary upwelling system, since nonlinear advection is important to the separation of the coastal jet and thus the formation of the anticyclone (Gan and Qu, 2008; Wang et al., 2006), which is familiar in the Gulf Stream separation problem (Haidvogel et al., 1992; Marshall and Tansley, 2001), an experiment without the nonlinear advection terms in the momentum equations was conducted [following, e.g., Gruber et al. (2011)]. It should be noted that the advection terms in the tracer equations are retained for transport of active and passive tracers (i.e., ecosystem variables). Hereafter, this experiment will be referred to as NO_ADV run.

3 Results

In this section, we first analyze the satellite-based observational data, focusing on the ~~spatio-temporal~~spatiotemporal covariance of wind, circulation, and biological production. After accessing the model performance against observation, we then describe and discuss the model results.

3.1 Spatio-temporal Analysis of Observation Data

Figure 2 shows the mean (Fig. 2a) and standard deviation (Fig. 2b) of surface ~~CHL~~chlorophyll overlaid with contours of mean ADT and KE respectively. In summer, the surface ~~CHL~~chlorophyll has a low concentration of <0.1 mg m^{-3} in the central SCS basin. By contrast, the ~~CHL~~chlorophyll is more than fivefold (>0.5 mg m^{-3}) along the southern Vietnamese coast. The high ~~CHL~~chlorophyll water appears to extend offshore following the coastal jet to the interior SCS. The jet overshoots after separating from the coast and bifurcates into a northeastward current and a quasi-stationary anti-cyclonic eddy (Fig. 2a). Centered at ~11° N near the tip of Vietnamese coast, high KE (>1.0 ~~m^{-2}~~m^2 s^{-2}) appears near the coast. The high variability of ~~CHL~~chlorophyll coincides with KE into the interior SCS, implying the contribution from the jet (Fig. 2b).

The box-averaged (magenta box in Fig. 2b) time-series of monthly UI, KE and NPP are shown in Fig. 3a-c; they show seasonal and interannual variations. KE ~~generally peaks in summer months, while~~ and NPP ~~has a~~both present biannually ~~signal~~signals in most years, i.e., peaks in summer and winter, as well as complex non-seasonal signals. Unsurprisingly, UI dominates about half (R^2=0.4548 for UI solely, $p<0.01$) of the total variability in NPP, which is consistent with studies in other wind-driven upwelling systems ~~(Gruber et al., 2011)~~(Gruber et al., 2011)~~,~~, and with the previous studies of the VBUS (Bombar et al., 2010; Voss et al., 2006). The correlation between KE and NPP is even higher (R^2=0.4930, $p<0.01$). Moreover, although KE could be dependent on the wind, the R^2 between KE and UI is 0.3240, suggesting that a large part (~68%) of the variation in KE is unexplained by the uniform alongshore wind. There are clear positive contributions to the biological production from both UI and KE. When KE ~~is~~and UI

are considered concurrently, additional ~15% of the variability in NPP is explained (R^2=0.6046, p<0.01). ~~Further investigation with 8-day mean NPP, UI, and KE after 60-day high-pass filter also shows a similar and significant relationship (despite the correlation is lower, R^2=0.1873, p<0.01, not presented in figures), demonstrating that the co-variation is robust not only for seasonal and longer time scales, but also for synoptic scale.~~

To further illustrate the modulation in the ecosystem by circulation, the high-NPP-anomaly (HNA) and low-NPP-anomaly (LNA) ~~periods of~~ currents were composited according to a non-seasonal NPP anomaly~~.~~ (Fig. 3c). The ~~climatological~~seasonal signal was firstly removed from the summertime NPP, yielding the non-seasonal NPP anomaly. The thresholds for HNA and LNA are defined as (above) 75% and (below) 25% percentile of the NPP anomaly, respectively. Different thresholds (60% and 70%) were also tested and very similar results can be seen. The velocity and direction for LNA, HNA and the normal state (i.e., neither LNA nor HNA) are respectively depicted in Fig. 4a-c, as well as the ADT difference between HNA and LNA (Fig. 4d). A student t-test suggests that the three circulation patterns are significantly (p<0.01) different. In contrast to the familiar separation and offshore jet pattern (Fig. 2a and Fig. 4c), the LNA circulation tends to flow along the coast without separation (Fig. 4a). On the other hand, the HNA circulation (Fig.4b) shows a clear separated jet and anticyclonic recirculating pattern south of the jet near 8.5° N, similar to the pattern seen during normal years (Fig. 4c); the flow speed is ~20% stronger than that of the normal state. Near the separation point, the HNA jet is more dissipated and slightly weakened compared with the LNA coastal jet. The KE averaged within the magenta box (Fig.2b) during the HNA state is 0.0827 $m^2\ s^{-2}$, which is ~65% larger than that during the LNA state (0.0502 $m^2\ s^{-2}$). The difference in flow patterns is consistent with a dipolar ADT difference, by which a westward (inverse to the jet) pressure gradient force anomaly is imparted to the flow (Fig. 4d), which is responsible for the jet separation process ~~(Batchelor, 1967; Gan and Qu, 2008). We now use~~(Batchelor, 1967; Gan and Qu, 2008). In order to examine the recirculation's role in the ecosystem, we now use the model to address the physical-biogeochemical coupling.

3.2 Model Validation

In Fig. 5, simulated SST and NPP are compared with observations. The model reproduces reasonably well the observed patterns of SST and NPP. In particular, the model captures the cross-shore SST gradient. The cold filament that overshoots from the coast to the interior of SCS is also clearly reproduced by the model. However, the modeled SST shows a systematic cold bias of ~1 °C, and the modeled NPP does not simulate well the ~~extreme~~extremely high values (>1000 mg C $m^{-2}\ d^{-1}$) along the Vietnamese coast. This may in part be attributed to overestimation of retrieved NPP near the coast ~~(e.g. Loisel et al., 2017)~~(Loisel et al., 2017). Off the coast, the model simulates well the ~~crossshore gradient of productivity. The gradient is generally high in areas influenced by the jet.~~ cross-shore gradient of productivity. The gradient is generally high in areas influenced by the jet. In the coupled model, while it is true that SST affects NPP through, for example, changes in the vertical stratification of the water column, both SST and NPP strongly depend on circulation (e.g. upwelling and/or downwelling), and in our case on the flow separation and KE also. In turn, the circulation is dominated by changes in the upper-layer depth (as diagnosed

through the SSH) and the horizontal gradients of SSH, and is much less dependent on the gradients of SST. Thus, the co-variation between the SST and ecosystem is largely controlled by the circulation. The dominant ecosystem response is the separation and non-separation contrast, which is captured well by the model (comparing Fig. 4 and Fig. 8).

Time series of modeled SST, surface KE and NPP, averaged over the magenta ~~box~~contour region (Fig.2b), are compared with observations in Fig. 6. Due in part to the realistic surface forcing and high resolution used, our model can reproduce the physical and biological ~~parameters~~variables in the VBUS. The ~~biannual signals~~seasonal cycles in all three quantities agree reasonably well with the observations. At interannual time scales, during the 2010 El Niño event, for example, monsoon was weaker (Fig. 3a), SST was warmer, and the KE was reduced. These features are simulated well, although the production drawdown is slightly weaker than the observation and the simulated SST under-estimates amplitude of the observed SST annual cycle by ~1.0 °C. For the surface current and productivity, our model shows excessive KE and insufficient production during winter, but the model-observation discrepancy is less notable in other seasons. The overestimated KE is partially contributed by the ~~ageostrophic (e.g., Ekman) components~~ component in ~~our~~the modeled surface current. Nevertheless, we can conclude that our model reasonably reproduced the temporal variability in the VBUS.

In addition, vertical profiles of the simulated NO_3 and ~~CHL~~chlorophyll, as two fundamental components of the marine ecosystem, are compared with observations (Fig. 7). The modeled NO_3 generally reflects the oligotrophic condition near the surface and the nutricline approximately at 50 m. Below the nutricline, the NO_3 profile shows moderate vertical gradient to the deep. The simulated NO_3 profile matches the observations remarkably well. For the ~~CHL~~chlorophyll, our model well simulates the concentration, not only at the surface but also in the deep layer. ~~Subsurface CHL~~A subsurface chlorophyll maxima appears at ~35 m, which is somewhat shallower than that in the observation~~.~~ (50 m). Except for model uncertainty, this discrepancy may also be related to the undersampling in observed profiles (no water samples between 25 m and 50 m depth). When chlorophyll is considered as a proxy of NPP, vertically integrated chlorophyll is more relevant. The vertical-averaged (5 m to 150 m) chlorophyll in the model and observation are 0.1595 and 0.1668 mg m^{-3}, respectively, which have a marginal difference (< 5%). Both the modeled and observed ~~CHL~~chlorophyll concentrations have a large range from 0 to >1.0 mg m^{-3} in the subsurface ~~CHL~~chlorophyll maxima. This reflects the large spatial variability in ~~CHL~~chlorophyll.

Following the analysis in Sect. 3.1, the multi-variable regression analysis on the model outputs were also conducted. The modeled NPP presents a phase lag with respect to the UI and KE variation. When NPP is lagged for one month, the correlation is 0.752 with a *p*-value of 0.0214, suggesting a significant regulation of the physical forcing to the productivity. Additionally, the composites of the HNA, LNA, and normal scenarios ~~(Fig. 8)~~(Fig. 6c) based on model outputs show contrasts among scenarios comparable to those in the observed cases in Fig. 4, further suggesting the reasonability of the model simulation~~.~~ (Fig. 8).

In summary, one could find that our model performs reasonably in reproducing the key ~~spatio-temporal~~spatiotemporal features in the hydrodynamics and ecosystem of VBUS. Inevitably, some discrepancies exist, which are less evident in the summer months. ~~Possible reasons for these discrepancies include insufficient~~

~~horizontal resolution, unrealistic parameterizations (e.g., turbulent mixing), inaccuracy in the atmospheric forcing, or uncertainties in the ecosystem parameters. Nevertheless, considering current focus are~~Nevertheless, considering the focus is to investigate the positive correlation between the productivity and the circulation, which was captured by the model (Fig. 8), these shortcomings ~~are~~could be accepted.

3.3 Analysis of Model Results

Modeled circulation and potential density from the multi-summer average are presented in Fig. 9a-d, with sea surface height overlaid. In the upwelling region, the doming of isopycnals (Fig. S2) is discernable as in the classical coastal upwelling models (O'Brien and Hurlburt, 1972). Consistent with previous studies, the coastal current flows northward along the shelf ~~(Hein et al., 2013)~~(Hein et al., 2013). The current also ~~dissipates~~disperses freshwater from the Mekong River, while the water seldom spreads away from the coast. The coastal current veers at ~11° N, directs offshore and then separates, forming the quasi-stationary anticyclone centered at ~110° E, 9° N. Near the core of the anticyclone, vigorous vertical motion near the surface can be found, implying submesoscale processes in play. Near 108° E, intensive onshore flow ascends on the slope. The high-density bottom water outcrops at 107-° E, rejoining the coastal water and directing north, thus forming a circuit.

The biogeochemical variables reveal that the ecosystem is largely controlled by the circulation (Fig. 9e-h, Fig. S2). Lateral nutrient gradient appears at the periphery of the anticyclone, which is characterized with depressed nitrate isosurface in the core and domed isosurface due to the upwelling and river injection near the coast (Fig. 9e). Stimulated by the river-injected and locally upwelled nutrient near the coast, primary production (PP) shows a surface maximum of >30 mg C m^{-3} d^{-1} (Fig. 9g). The water with high production is then advected offshore by the jet (Fig. 9h), leading to an offshore bloom patch in a curved shape which is familiar in the Vietnam coast (e.g., Fig. 5c). The jet also conveys the water with high particulate organic carbon ~~(POC)~~ offshore. The distribution of ~~POC~~particulate organic carbon is somewhat deeper and more ~~dissipated~~spread than that of high PP water, suggesting the vertical sinking and lateral transport processes ~~(Nagai et al., 2015)~~(Nagai et al., 2015). Remineralization of ~~POC~~organic carbon results in a subsurface ammonium maximum at ~50 m (Fig. 9f) consistent with ~~the study~~other studies in SCS ~~(Li et al., 2015)~~(Li et al., 2015). Part of the ammonium could then fuel nitrification and production, while the rest rejoins the circulation with the upwelling water in the bottom Ekman layer. In summary, the model outputs clearly reveal circuiting circulation and cycled ecosystem, which will be further discussed in Sect. 4.

4 Discussion

4.1 Biogeochemical Cycle in VBUS

~~Via analysis on satellite data and model outputs, consistent and robust positive contribution from the local circulation to the biological production was revealed, in addition to the contribution from the wind, in the summer~~

~~VBUS system. The contribution of the circulation is distinct from the major coastal upwelling systems, where the offshore transport by the mean current appears to suppress the production by reducing the nearshore nutrient inventory (Gruber et al., 2011; Nagai et al., 2015).~~

~~Comparing the ecosystems in LNA and HNA (Fig. 10~~In the summer VBUS system, it is generally agreed that the wind's predominant role in controlling the variability in the production of VBUS, especially on the inter-annual scale (Dippner et al., 2013). This is also the case in our analysis where UI contributes ~45% of the total variability in production. In addition, via analysis of satellite data and model outputs, consistent and robust positive contribution from the local circulation to the biological production was also revealed. The contribution of the circulation is distinct from the major coastal upwelling systems, where the offshore transport by the mean current appears to suppress the production by reducing the nearshore nutrient inventory (Gruber et al., 2011; Nagai et al., 2015). The separated current system was considered to transport high-chlorophyll water offshore (Xie et al., 2003). In the offshore region, the production appeared to be elevated (Bombar et al., 2010). However, the fate of the offshore nutrients was rarely investigated in the literature.

Comparing the ecosystems in LNA and HNA (Fig. 10), the following stages of the cycle can be deduced: (1) The upwelled and riverine input nutrient (majorly inorganic) stimulate high production near the Vietnam coast~~.~~ (Dippner et al., 2007); (2) The produced organic matters are transported offshore by the jet; The water has high ~~CHL~~chlorophyll (e.g., Fig. 2a) and high organic matters (Fig. 9h) in the euphotic zone; (3) A significant portion of the nutrient (majorly in organic form) is transported back to the south of VBUS by the westward recirculation. The quasi-stationary rotating anticyclone impedes further offshore leakage of the nutrients (Fig. 10~~).~~i). (4) The trapped organic matters are remineralized, forming the subsurface maxima of ammonium (Fig. 9f, which supports regeneration production with an *f*-ratio of ~60%, Table 1) and replenishing the nitrate by nitrification. ~~Afterwards~~The offshore remineralization can be supported by the high oxygen consumption found off Vietnamese coasts (Jiao et al., 2014). Afterward, the nutrients are upwelled by bottom Ekman pumping (see high nutrient in the bottom boundary layer in Fig. 9e) and wind-induced upwelling, and finally rejoin in the local biogeochemical cycle. ~~The speed of this cycle plays~~The recirculation may determine the available nutrient inventory, therefore playing a significant role in controlling the productivity, which will be further supported by the experiment in the following section.

4.2 Dynamic Analysis

By controlling the available nutrients, the ~~circulation largely determines~~recirculation modulates the ~~speed of the biogeochemical cycle.~~productivity in VBUS. The influence of the ~~circulation~~recirculation is further elucidated below. Table 1 summarizes the difference of the ecosystems in the standard run and NO_ADV experiment. The NO_ADV experiment can be regarded as an extreme case where the circulation shows very weak tendency of separation (also see Fig. S1). The horizontal and vertical fluxes of nitrate in three scenarios are also depicted in Fig. 11.

In the VBUS, the availability of nutrients principally controls the productivity ~~(Hein et al., 2013)~~(Hein et al., 2013). Considering a quasi-steady state of nutrient in a coastal region, river-injected and upward inputted nutrient should be counter-balanced by vertical export production and lateral exchanges. The lateral exchanges include both advection and diffusion, while it was pointed out that horizontal mixing is one or two order-of-magnitude lower than that of horizontal advection ~~(Lu et al., 2015)~~(Lu et al., 2015). Hence, as a sink term, the lateral exchanges are determined mostly by the advective fluxes normal to the boundary of the predefined box. Diagnostic also suggests a dominance role of advection process in the vertical over mixing. Given the fact the standard run and NO_ADV experiment ~~has~~have the same riverine input and similar export flux, one could infer that the difference between two model cases is largely due to the different lateral transports and upwelled fluxes of nutrients.

In the LNA (Fig. 4a and Fig. 8a) and also in the NO_ADV experiment (Fig. S1), the circulation pattern switches to the along-isobath pattern, which modifies the local biogeochemical cycle. More nutrient is transported northward and offshore out of VBUS and never comes back, leading to a reduction of nutrient (Fig. 11). This effect can be demonstrated by cross-section nutrient flux across 109° E section. The more nutrient leakage, the less westward nutrient flux across this section. In NO_ADV run, the westward flux of nitrate is significantly reduced by 36.2% (Table 1). The reduction of nutrient is accompanied with suppressed the upward nutrient flux (-46.5~~-~~%) near the shelf edge (~100 m). As a consequence of more leakage and less upwelling influx, the nitrate reservoir and new production are significantly reduced by 20.7 % and 21.9 %, significantly inhibiting the primary production process (15.7 %, Table 1). Other ecosystem constituents decrease to a limit degree, such as -2.6% for ammonium, and -3.0% for DOC. This interpretation is further supported by the post-El Niño scenario. In 2010, more significant suppression occurs in the vertical nutrient flux (-99.6%), while the horizontal fluxes also respond to decrease. Due to the drawdown in the wind-induced upwelling and ~~-~~recirculation (Table 1), the production is extremely low in summer 2010 (Fig. 3c).

~~The more intensive separation, the larger KE in VBUS, and vice versa. The accelerated coastal current is also associated with intensified cross isobath transport by bottom Ekman effect (Gan et al., 2009). Hence, high KE is linked to accelerated biogeochemical cycle. Combining all the effects, the intensified circulation is a condition favorable for the nutrient inventory, and hence the productivity, especially during relatively low KE scenarios.~~

The larger KE, the more intensive separation, and vice versa (see Appendix B for additional discussion about this point). This separation was similar to the Gulf Stream detachment problem in many aspects. In particular, various factors could affect the intensity and position of the separation (Chassignet and Marshall, 2008). Generally, the mechanism of the current separation was considered to be ascribed to the wind stress curl (Xie et al., 2003). We also found that the current separation was very sensitive to the wind stress curl (not shown in figures). Hence, one may argue that this co-variability is controlled by the variation of wind-forcing. However, as mentioned in Sect. 3.1, a large part (~68%) of the variation in KE is unexplained by the large-scale wind. In addition, our sensitivity experiments without the nonlinear advection of momentum showed very weak separation, in agreement with that of Wang et al. (2006). This implies wind-forcing is not the only factor in controlling the current system, while the intrinsic dynamics are also important. The accelerated coastal current is also associated with intensified cross-

isobath transport by bottom Ekman effect (Gan et al., 2009) or dynamic upwelling (Yoshida and Mao, 1957) due to the rotational current (Dippner et al., 2007). Hence, low KE reduces the recirculation of nutrients. Combining all the effects, the intensified current is a condition favorable for the nutrient inventory, and hence the productivity. To a larger scale, the recirculation current couples coastal upwelling and offshore region in the major coastal upwelling systems, e.g., in the Canary basin (Pelegrí et al., 2005). In this study, this effect was also found to be important, which may contribute up to 15% of the productivity variability.

5 Conclusions

Via analyzing the summertime remote sensing data in the VBUS, a tight ~~spatio-temporal~~spatiotemporal covariation between the ecosystem and near-surface circulation was revealed. The water with high kinetic energy appeared to coincide with high ~~CHL~~chlorophyll variability. Statistical analysis suggested that the high level of productivity was associated with the high level of circulation intensity, which accounted for ~15% of the variability in productivity. Elevated kinetic energy and intensified circulation were related with the separation of the upwelling current system. Especially, in the low-productivity scenarios, the circulation pattern shifts from the intensive separation pattern to a moderate alongshore non-separated pattern.

To further investigate the linkage between the circulation and the ecosystem, a physical-biological coupled model was ~~configurated. Numerical experiment was designed to reproduce the non-separated circulation pattern, while maintaining the external monsoon forcing.~~developed. The modeled results were validated favorably compared with the remote sensing and *in- situ* observation data. In particular, model reproduced the positive contribution from the circulation intensity to the productivity. A numerical experiment was also designed to reproduce the weak-separated circulation pattern without the recirculation, while maintaining the external monsoon forcing.

Inspection into the model results highlighted the ~~circulation's~~recirculation's role in the local biogeochemical cycle. As presented in the schematic diagram in Fig. 12, the separated circulation and resultant ~~quasi-stationary anticyclone~~ recirculation were favorable for the ~~recirculation of nutrients~~nutrient inventory. During non-separation scenarios, the nutrients northward transported by the alongshore current would never come back, leading to a nutrient leakage. The nutrient leakage further induced the feedback summarized in Fig. 12b, which could reduce the nitrate inventory by ~21% and the NPP by ~16% in the experiment representative for very weak separation. The weakened coastal current was also associated with reduced ~~bottom Ekman transport~~dynamic upwelling, hence further reducing the vertical flux of nutrient. ~~As the KE increasing, the biogeochemical cycle was accelerated.~~ This resulted in the positive ~~correlation~~contribution to the productivity.

This finding provides a new insight into the complex physical-biological coupling in the Vietnam coastal upwelling system. Moreover, this understanding could help to predict the future reaction of productivity in the SCS. ~~As revealed by Yang and Wu (2012)~~As revealed by Yang and Wu (2012), the summertime near-surface circulation of SCS had experienced a long-term trend of being more energetic, characterized with intensified separation and recirculation in the VBUS (see their figure 9). Whether this long-term trend of circulation will also induce a

potential trend in the ecosystem in response to future climate changes is a topic of common interests, which merits further investigation.

6 Data Availability

The CCMP gridded Ocean Surface Wind Vector L3.0 First-Look Analyses (Version 1) data was accessed [2015-03-12] at http://dx.doi.org/10.5067/CCF30-01XXX. The MODIS Aqua Level 3 ~~CHL~~chlorophyll data was accessed [2014-05-16] at http://oceancolor.gsfc.nasa.gov. The VGPM NPP data was available at http://www.science.oregonstate.edu/ocean.productivity/index.php. Gridded monthly-mean ADT, available at http://www.aviso.altimetry.fr/en/data/products/sea-surface-height-products/global/, was produced by Ssalto/Duacs (http://www.aviso.oceanobs.com/duacs/), and was distributed by Aviso with support from the Centre National d'Etudes Spatiales (*Cnes*). The OISST data was obtained from the National Climatic Data Center of NOAA (https://www.ncdc.noaa.gov/oisst/data-access).

Appendix A: Abbreviations

In Table A1, all the acronyms in the paper were listed.

Table A1 List of Acronyms

~~*Locations*~~Acronym	Definition	~~*Variables*~~Acronym	Definition
SCS	South China Sea	~~CHL~~NPP	~~chlorophyll a~~vertical-integrated Net Primary Production
VBUS	Vietnam Boundary Upwelling System	~~NPP~~PP	~~vertical integrated net primary production~~Primary Production (as a function of depth)
~~*Data and Methods*~~		~~PP~~	~~primary production (as a function of depth)~~
CCMP	Cross-Calibrated Multi-Platform data	~~UI~~KE	kinetic energy~~upwelling intensity~~
MODIS	Moderate Resolution Imaging Spectroradiometer data	TFOR~~KE~~	Taiwan Strait Nowcast\Forecast system~~kinetic energy~~
~~NCEP~~	~~National Centers for Environmental Prediction~~	~~POC~~	~~particulate organic carbon~~
VGPM	chlorophyll-based Vertically Generalized Production Model	~~*Modeling*~~CoSINE	Carbon, Silicon, Nitrogen Ecosystem model
ADT	Absolute Dynamic Topography	NO_ADV~~TFOR~~	model experiment with no advection term in momentum equations~~Taiwan Strait Nowcast\Forecast system~~
OISST	Optimum Interpolation Sea Surface Temperature	~~CoSINE~~UI	Upwelling Intensity~~Carbon, Silicon, Nitrogen Ecosystem model~~
HNA/LNA	high/low-NPP anomaly scenario	~~NO_ADV~~	~~model experiment with no advection term in momentum equations~~

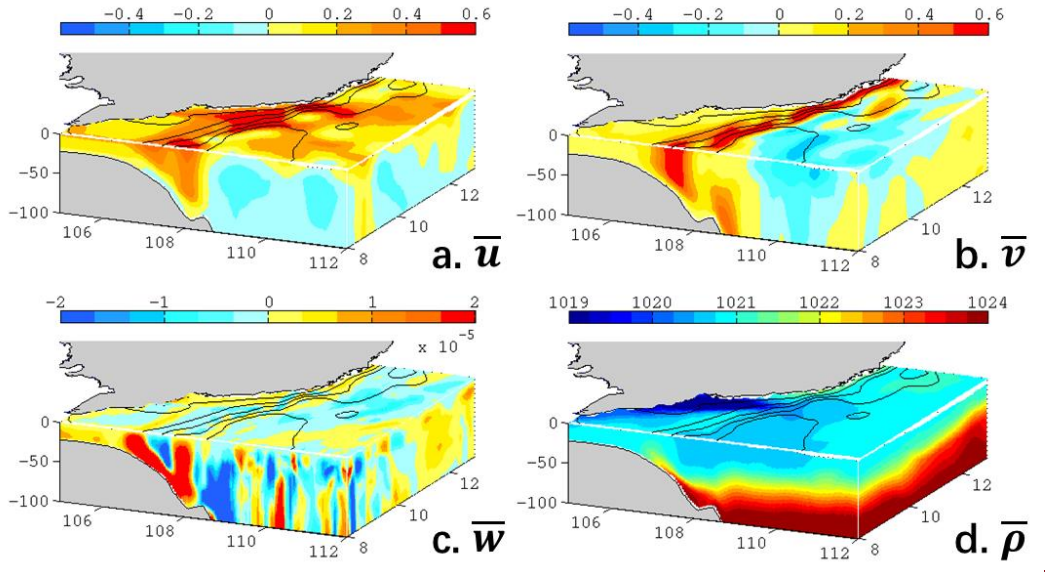

Appendix B: Flow Separation and Kinetic Energy

Qualitatively, both the analysis based on remote sensing data and model results suggest the separation flow is linked with stronger KE (~65% larger in HNA case then LNA case, Sect. 3.1). Moreover, a separation index (SI) is defined to quantitatively explain the relation between the flow separation and intensified circulation. The SI can be written as:

$$SI = \sum \frac{u \cdot \cos\varphi + v \cdot \sin\varphi}{\sqrt{u^2 + v^2}}, \quad \text{(A1)}$$

Where u and v are the two surface velocity components, and φ is the angle between the topography gradient and the positive x-axis. This SI is essentially the area-averaged cross-isobath velocity normalized by the magnitude of the velocity, which is used to quantify flow separation here.

Fig. A1 shows the spatial distribution of SI in Aug 2010. The positive values indicate the flow is downslope while negatives suggest ascent. Large SI can be observed near the separation point ~11.5°N. Taking spatial average over the box region in Fig. A1, a generally good positive correlation ($R=0.7175$, $p<0.01$) between log(KE) and SI is found (see Fig. A2). The log(KE) and SI presents a logistic-type relationship, where SI asymptotically approaches a maximum value of ~0.35. This suggests that the strong flow separation and elevated KE are tightly linked. Further, from the scatter plot of KE vs. SI (Fig. A2), we find that 0.1 m^2s^{-2} is a critical value, which divides the data into two subsets while minimizes the slope of the right part (blue fitting curve in Fig. A2).

Fig. A1 shows the distribution of SI in Aug 2010. Positive values indicate that the flow is separating and downslope, and that may be seen off Vietnam south of the coastline bend. Large SI (~1.0) can be observed near the separation

point ~11.5°N. Taking spatial average over the box region in Fig. 2a or Fig. A1, there is a good positive correlation (R=0.7175, p<0.01) between log(KE) and SI (see Fig. A2). Moreover, SI may be seen to generally increase with KE to a value of 0.25~0.3 and then it levels off (i.e. the slope becomes less) – see the red and blue lines in Fig. A2. The log(KE) and SI thus appear to show a logistic-type behavior, in which SI asymptotically approaches some maximum value (in this case ~0.3). This suggests that the strong flow separation and elevated KE are tightly linked. From Fig. A2, the value of KE ≈ 0.1 m^2s^{-2} appears to be a critical value.

Dynamically, the nonlinear advection term in the momentum equation can be written as the vector invariant form [see e.g. (Gill, 1982)]:

$$\vec{u}\cdot\nabla\vec{u} = (\nabla\times\vec{u})\times\vec{u} + \nabla(\frac{1}{2}\left|\vec{u}\right|^2), \quad \text{(A2)}$$

This decomposition directly links the nonlinear advection term and the gradient of KE (which scales KE over a length scale L). Meanwhile, the nonlinear advection is an important mechanism in driving flow separation [see, for instance, Oey et al. (2014)]. Stronger advection suggests intense cross isobath flow. Therefore, a dynamic linkage between the flow separation and the intensified KE and circulation can also be established, further supporting this argument.

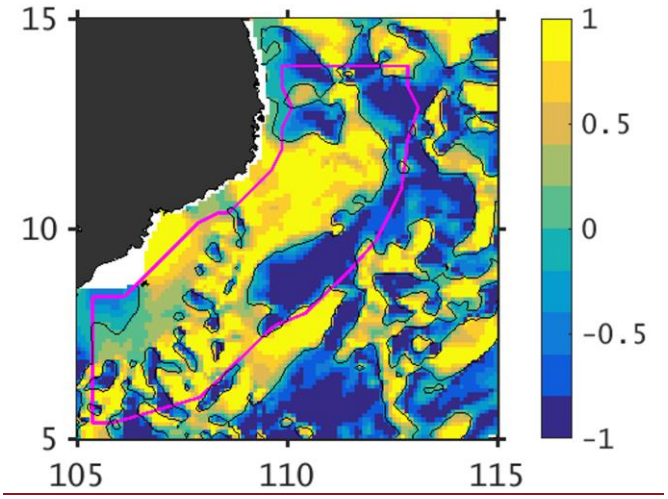

Figure A1 Example of modeled SI in Aug 2010.

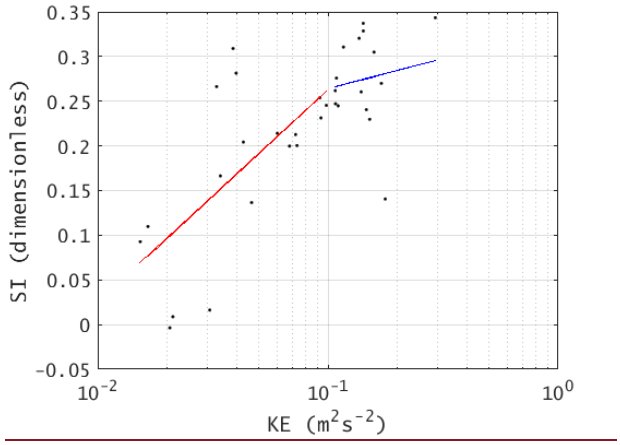

Figure A2 Summer-month (MJJAS) KE vs SI averaged over the box region in Fig. A1 (overall R=0.7175, p<0.01).

Supplementary Figures:

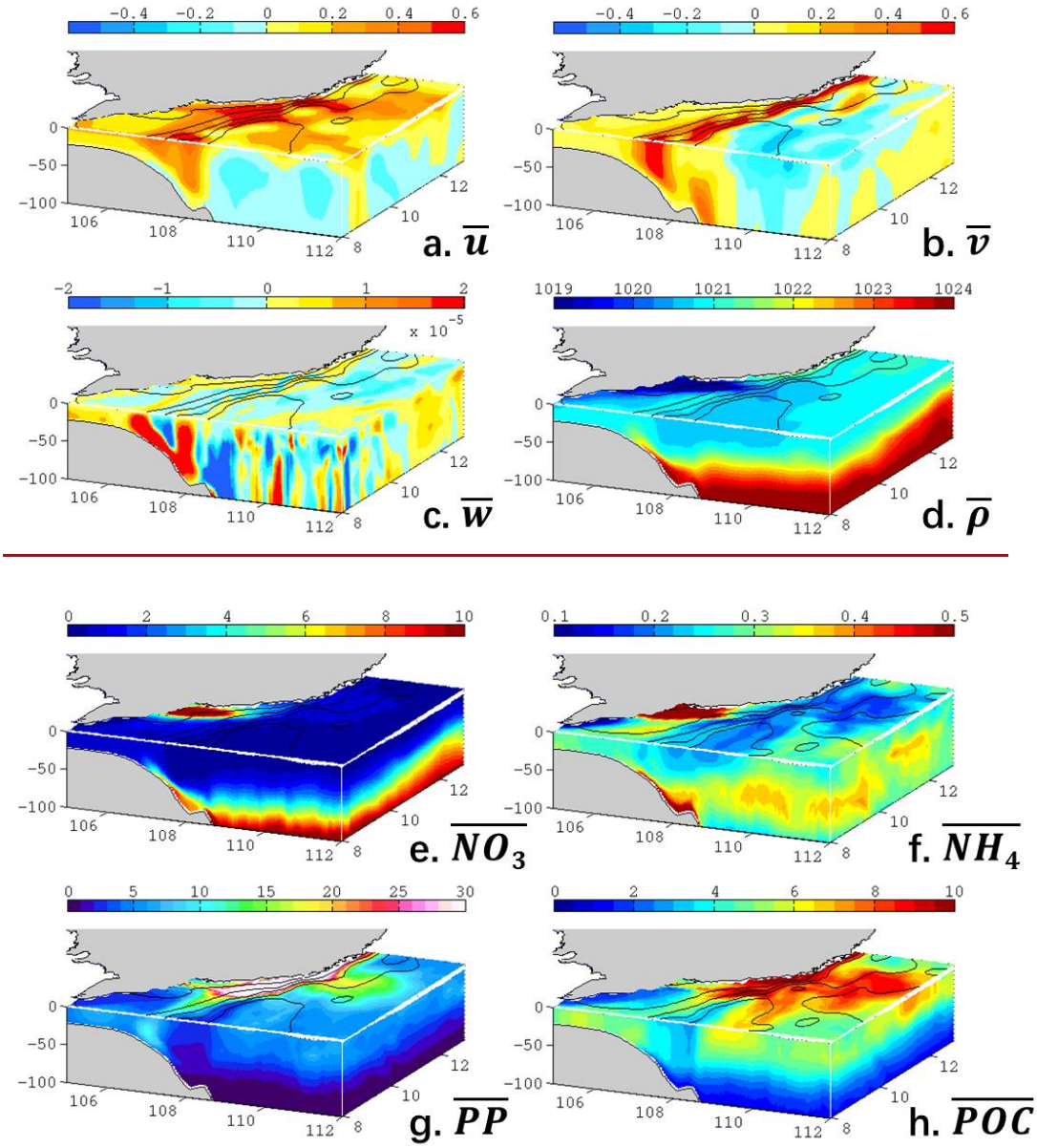

Figure S1 Same with Fig. 9, but for NO_ADV model run. (a) Zonal velocity in m s^{-1}, (b) meridional velocity in m s^{-1}, (c) vertical velocity in m s^{-1}, (d) potential density in kg m^{-3}, (e) nitrate in mmol m^{-3}, (f) ammonium in mmol m^{-3}, (g) primary production in mg C m^{-3} d^{-1}, and particulate organic carbon in mmol C m^{-3}. Overlapped contours are the mean sea level (every 0.1 m).

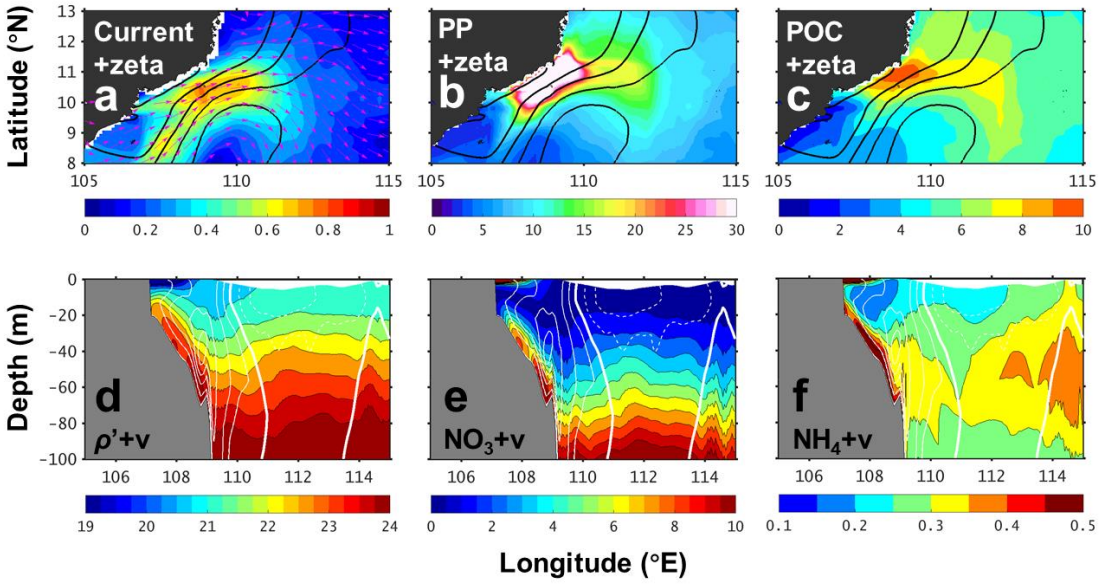

Figure S2 (a-c) Modeled sea level (black contour, CI=0.1 m) overlaid with (a) surface current (color: magnitude in m s^{-1}; vector: flow direction), (b) surface primary production (mg C m^{-3} d^{-1}), and (c) particulate organic carbon (mmol C m^{-3}). (d-f) Sections along 10° N: meridional velocity (positive in solid contours and negative in dashed, CI=0.1 m s^{-1}. Thick contours indicate zero value) overlaid with (d) potential density anomaly, (e) nitrate concentration (mmol m^{-3}), and (f) ammonia concentration (mmol m^{-3}).

Acknowledgements

This study was supported by grant No.2016YFA0601201 from the Ministry of Science and Technology of the People's Republic of China (MOST), and grants U1305231, 41476005, 41476007 and 41630963 from the National Natural Science Foundation of China (NSFC).

References

Atlas, R., Hoffman, R. N., Ardizzone, J., Leidner, S. M., Jusem, J. C., Smith, D. K., and Gombos, D.: A cross-calibrated, multiplatform ocean surface wind velocity product for meteorological and oceanographic applications, Bull. Am. Meteorol. Soc., 92, 157-174, 2011.

Bakun, A.: Coastal upwelling indices, west coast of North America, 1946-71, US Dept. Commerce NOAA Tech. Rep. NMFS-SSRF, 671, 1-103, 1973.

Bakun, A.: Patterns in the ocean: ocean processes and marine population dynamics, California Sea Grant, in cooperation with Centro de Investigaciones Biologicas del Noroeste, La Paz, Mexico, 1996.

Batchelor, G. K.: An Introduction to Fluid Dynamics, Cambridge University Press, New York, 1967.

~~Banzon, V., Smith, T. M., Chin, T. M., Liu, C., and Hankins, W.,: A long-term record of blended satellite and in situ sea-surface temperature for climate monitoring, modeling and environmental studies. Earth Syst. Sci. Data, 8, 165–176, doi:10.5194/essd-8-165-2016, 2016.~~

Behrenfeld, M. J. and Falkowski, P. G.: Photosynthetic rates derived from satellite-based chlorophyll concentration, Limnol. Oceanogr., 42, 1-20, 1997.

Bombar, D., Dippner, J. W., Doan, H. N., Ngoc, L. N., Liskow, I., Loick-Wilde, N., and Voss, M.: Sources of new nitrogen in the Vietnamese upwelling region of the South China Sea, J. Geophys. Res., 115, 2010.

Bombar, D., Moisander, P. H., Dippner, J. W., Foster, R. A., Voss, M., Karfeld, B., and Zehr, J. P.: Distribution of diazotrophic microorganisms and nifH gene expression in the Mekong River plume during intermonsoon, Marine Ecology Progress Series, 424, 39-52, 2011.

Bryan, F. O., Hecht, M. W., and Smith, R. D.: Resolution convergence and sensitivity studies with North Atlantic circulation models. Part I: The western boundary current system, Ocean Model, 16, 141-159, 2007.

Chai, F., Liu, G., Xue, H., Shi, L., Chao, Y., Tseng, C.-M., Chou, W.-C., and Liu, K.-K.: Seasonal and interannual variability of carbon cycle in South China Sea: A three-dimensional physical-biogeochemical modeling study, J. Oceanogr., 65, 703-720, 2009.

Chassignet, E. P. and Marshall, D. P.: Gulf Stream separation in numerical ocean models, 177, 39-61, 2008.

Chen, G., Xiu, P., and Chai, F.: Physical and biological controls on the summer chlorophyll bloom to the east of Vietnam, J. Oceanogr., 70, 323-328, 2014.

Chen, Z., Yan, X.-H., Jo, Y.-H., Jiang, L., and Jiang, Y.: A study of Benguela upwelling system using different upwelling indices derived from remotely sensed data, Cont. Shelf Res., 45, 27-33, 2012.

~~Dai, A., Qian, T., Trenberth, K. E., and Milliman, J. D.: Changes in continental freshwater discharge from 1948 to 2004, J. Clim., 22, 2773-2792, 2009.~~

Cushing, D.: Upwelling and fish production, FAO Fish. Tech. Pap, 84, 40, 1969.

Dippner, J. W., Bombar, D., Loick‐Wilde, N., Voss, M., and Subramaniam, A.: Comment on "Current separation and upwelling over the southeast shelf of Vietnam in the South China Sea" by Chen et al, J. Geophys. Res. Oceans, 118, 1618-1623, 2013.

Dippner, J. W., Nguyen, K. V., Hein, H., Ohde, T., and Loick, N.: Monsoon-induced upwelling off the Vietnamese coast, Ocean Dyn., 57, 46-62, ~~2006~~2007.

Doan-Nhu, H., Lam, N.-N., and Dippner, J. W.: Development of Phaeocystis globosa blooms in the upwelling waters of the South Central coast of Viet Nam, J. Mar. Syst., 83, 253-261, 2010.

Ekman, V. W.: On the influence of the earth's rotation on ocean-currents, Arkiv. Mat. Astron. Fys., 211, 1-52, 1905.

Gan, J., Cheung, A., Guo, X., and Li, L.: Intensified upwelling over a widened shelf in the northeastern South China Sea, J. Geophys. Res., 114, 2009.

Gan, J. and Qu, T.: Coastal jet separation and associated flow variability in the southwest South China Sea, Deep Sea ~~Res.~~Research Part I: Oceanographic Research Papers, 55, 1-19, 2008.

Gill, A. E.: Atmosphere-ocean dynamics, Academic press, 1982.

Griffies, S. M. and Hallberg, R. W.: Biharmonic Friction with a Smagorinsky-Like Viscosity for Use in Large-Scale Eddy-Permitting Ocean Models, Monthly Weather Review, 128, 2935-2946, 2000.

Gruber, N., Lachkar, Z., Frenzel, H., Marchesiello, P., Munnich, M., McWilliams, J. C., Nagai, T., and Plattner, G.-K.: Eddy-induced reduction of biological production in eastern boundary upwelling systems, Nature Geosci, 4, 787-792, 2011.

Guo, M., Chai, F., Xiu, P., Li, S., and Rao, S.: Impacts of mesoscale eddies in the South China Sea on biogeochemical cycles, Ocean Dyn., doi: 10.1007/s10236-015-0867-1, 2015. 2015.

Haidvogel, D. B., McWilliams, J. C., and Gent, P. R.: Boundary Current Separation in a Quasigeostrophic, Eddy-resolving Ocean Circulation Model, J. Phys. Oceanogr., 22, 882-902, 1992.

Hein, H., Hein, B., Pohlmann, T., and Long, B. H.: Inter-annual variability of upwelling off the South-Vietnamese coast and its relation to nutrient dynamics, Global Planet. Change, 110, 170-182, 2013.

Isoguchi, O. and Kawamura, H.: MJO-related summer cooling and phytoplankton blooms in the South China Sea in recent years, Geophys. Res. Lett., 33, 2006.

Jiang, Y. W., Chai, F., Wan, Z. W., Zhang, X., and Hong, H. S.: Characteristics and mechanisms of the upwelling in the southern Taiwan Strait: a three-dimensional numerical model study, J. Oceanogr., 67, 699-708, 2011.

Jiao, N., Zhang, Y., Zhou, K., Li, Q., Dai, M., Liu, J., Guo, J., and Huang, B.: Revisiting the CO2 "source" problem in upwelling areas: a comparative study on eddy upwellings in the South China Sea, Biogeosciences, 11, 2465-2475, 2014.

Kalnay, E., Kanamitsu, M., Kistler, R., Collins, W., Deaven, D., Gandin, L., Iredell, M., Saha, S., White, G., and Woollen, J.: The NCEP/NCAR 40-year reanalysis project, Bull. Am. Meteorol. Soc., 77, 437-471, 1996.

Kuo, N.-J., Zheng, Q., and Ho, C.-R.: Response of Vietnam coastal upwelling to the 1997–1998 ENSO event observed by multisensor data, Remote Sens. Environ., 89, 106-115, 2004.

Kuo, N.-J., Zheng, Q., and Ho, C.-R.: Satellite observation of upwelling along the western coast of the South China Sea, Remote Sens. Environ., 74, 463-470, 2000.

Kuo, N. J. and Ho, C. R.: ENSO effect on the sea surface wind and sea surface temperature in the Taiwan Strait, Geophys. Res. Lett., 31, 2004.

Large, W. G., McWilliams, J. C., and Doney, S. C.: Oceanic vertical mixing: A review and a model with a nonlocal boundary layer parameterization, Rev. Geophys., 32, 363-404, 1994.

Li, Q. P., Wang, Y., Dong, Y., and Gan, J.: Modeling long-term change of planktonic ecosystems in the northern South China Sea and the upstream Kuroshio Current, J. Geophys. Res. Oceans, 120, 3913-3936, 2015.

Liao, E., Jiang, Y., Li, L., Hong, H., and Yan, X.: The cause of the 2008 cold disaster in the Taiwan Strait, Ocean Model, doi: 10.1016/j.ocemod.2012.11.004, 2013. 1-10, 2013.

Lin, X., Yan, X.-H., Jiang, Y., and Zhang, Z.: Performance assessment for an operational ocean model of the Taiwan Strait, Ocean Model, 102, 27-44, 2016.

Liu, G. and Chai, F.: Seasonal and interannual variability of primary and export production in the South China Sea: a three-dimensional physical-biogeochemical model study, ICES J. Mar. Sci., 66, 420-431, 2009.

Liu, K.-K., Atkinson, L., Quinones, R., and Talaue-McManus, L.: Carbon and nutrient fluxes in continental margins: a global synthesis, Springer Science & Business Media, 2010.

Liu, K~~.~~-K., Chao, S. Y., Shaw, P. T., Gong, G. C., Chen, C. C., and Tang, T. Y.: Monsoon-forced chlorophyll distribution and primary production in the South China Sea: observations and a numerical study, Deep-Sea ~~Research~~Res. Part I-~~Oceanographic Research Papers,~~Oceanogr. Res. Pap., 49, 1387-1412, 2002.

Liu, W. T., Katsaros, K. B., and Businger, J. A.: Bulk parameterization of air-sea exchanges of heat and water vapor including the molecular constraints at the interface, J. Atmos. Sci., 36, 1722-1735, 1979.

Liu, X., Wang, J., Cheng, X., and Du, Y.: Abnormal upwelling and chlorophyll-aconcentration off South Vietnam in summer 2007, J. Geophys. Res. Oceans, 117~~, n/a-n/a~~, 2012.

Loick-Wilde, N., Bombar, D., Doan, H. N., Nguyen, L. N., Nguyen-Thi, A. M., Voss, M., and Dippner, J. W.: Microplankton biomass and diversity in the Vietnamese upwelling area during SW monsoon under normal conditions and after an ENSO event, Prog. Oceanogr., 153, 1-15, 2017.

Loisel, H., Vantrepotte, V., Ouillon, S., Ngoc, D. D., Herrmann, M., Tran, V., Mériaux, X., Dessailly, D., Jamet, C., Duhaut, T., Nguyen, H. H., and Van Nguyen, T.: Assessment and analysis of the chlorophyll-a concentration variability over the Vietnamese coastal waters from the MERIS ocean color sensor (2002–2012), Remote Sens. Environ., 190, 217-232, 2017.

Lu, W., Yan, X.-H., Han, L., and Jiang, Y.: One-dimensional ocean model with three types of vertical velocities: a case study in the South China Sea, Ocean Dyn., doi: 10.1007/s10236-016-1029-9, 2017. 1-10, 2017.

Lu, W., Yan, X.-H., and Jiang, Y.: Winter bloom and associated upwelling northwest of the Luzon Island: A coupled physical-biological modeling approach, J. Geophys. Res. Oceans, 120, 533-546, 2015.

Ma, W., Chai, F., Xiu, P., Xue, H., and Tian, J.: Modeling the long-term variability of phytoplankton functional groups and primary productivity in the South China Sea, J. Oceanogr., 69, 527-544, 2013.

Ma, W., Chai, F., Xiu, P., Xue, H., and Tian, J.: Simulation of export production and biological pump structure in the South China Sea, Geo-Mar. Lett., 34, 541-554, 2014.

Marshall, D. P. and Tansley, C. E.: An Implicit Formula for Boundary Current Separation, J. Phys. Oceanogr., 31, 1633-1638, 2001.

Mittelstaedt, E.: Upwelling regions, Landoldt-Börnstein, New Series, 3, 135-166, 1986.

Nagai, T., Gruber, N., Frenzel, H., Lachkar, Z., McWilliams, J. C., and Plattner, G. K.: Dominant role of eddies and filaments in the offshore transport of carbon and nutrients in the California Current System, J. Geophys. Res. Oceans, 120, 5318-5341, 2015.

O'Brien, J. J. and Hurlburt, H.: A numerical model of coastal upwelling, J. Phys. Oceanogr., 2, 14-26, 1972.

Oey, L.-Y., Chang, Y.-L., Lin, Y.-C., Chang, M.-C., Varlamov, S., and Miyazawa, Y.: Cross flows in the Taiwan Strait in winter, J. Phys. Oceanogr., 44, 801-817, 2014.

Pelegrí, J. L., Arístegui, J., Cana, L., González-Dávila, M., Hernández-Guerra, A., Hernández-León, S., Marrero-Díaz, A., Montero, M. F., Sangrà, P., and Santana-Casiano, M.: Coupling between the open ocean and the coastal upwelling region off northwest Africa: water recirculation and offshore pumping of organic matter, J. Mar. Syst., 54, 3-37, 2005.

Shchepetkin, A. and McWilliams, J.: The regional oceanic modeling system (ROMS): a split-explicit, free-surface, topography-following-coordinate oceanic model, Ocean Model, 9, 347-404, 2005.

Tang, D. L., Kawamura, H., Doan-Nhu, H., and Takahashi, W.: Remote sensing oceanography of a harmful algal bloom off the coast of southeastern Vietnam, J. Geophys. Res. Oceans, 109, 2004.

Voss, M., Bombar, D., Loick, N., and Dippner, J. W.: Riverine influence on nitrogen fixation in the upwelling region off Vietnam, South China Sea, Geophys. Res. Lett., 33, 2006.

Wang, G., Chen, D., and Su, J.: Generation and life cycle of the dipole in the South China Sea summer circulation, J. Geophys. Res., 111, 2006.

Wang, J., Hong, H., Jiang, Y., Chai, F., and Yan, X.-H.: Summer nitrogenous nutrient transport and its fate in the Taiwan Strait: A coupled physical-biological modeling approach, J. Geophys. Res. Oceans, 118, 4184-4200, 2013.

Wong, G. T. F., Ku, T. L., Mulholland, M., Tseng, C. M., and Wang, D. P.: The SouthEast Asian time-series study (SEATS) and the biogeochemistry of the South China Sea - An overview, Deep Sea Res. Part II, 54, 1434-1447, 2007.

Wyrtki, K.: Physical Oceanography of the Southeast Asian waters. 1961.

Xie, S.-P., Hu, K., Hafner, J., Tokinaga, H., Du, Y., Huang, G., and Sampe, T.: Indian Ocean capacitor effect on Indo-western Pacific climate during the summer following El Niño, J. Clim., 22, 730-747, 2009.

Xie, S. P., Xie, Q., Wang, D., and Liu, W. T.: Summer upwelling in the South China Sea and its role in regional climate variations, J. Geophys. Res. Oceans, 108, 2003.

Xiu, P. and Chai, F.: Connections between physical, optical and biogeochemical processes in the Pacific Ocean, Prog. Oceanogr., 122, 30-53, 2014.

Xu, X., Qiu, Z., and Chen, H.: The general descriptions of the horizontal circulation in the South China Sea, 1982, 137-145.

Yang, H. and Wu, L.: Trends of upper-layer circulation in the South China Sea during 1959-2008, J. Geophys. Res. Oceans, 117, 2012.

Yoshida, K. and Mao, H.-L.: A theory of upwelling of large horizontal extent, J. Mar. Syst., 16, 40-54, 1957.

Table

650 **Table 1 Summery of the ecosystems in three model scenarios**

Quantities integrated over top 100 m of the box region (Fig. 2b)	~~Standard~~Normal years (except 2010)	NO_ADV	2010 post-El Niño
NO_3 ($\times 10^9$ mol)	11.3	8.96 (-20.7%)	10.71 (-5.2%)
NH_4 ($\times 10^9$ mol)	1.52	1.48 (-2.6%)	1.51 (-0.7%)
DOC ($\times 10^9$ mol C)	234	227 (-3.0%)	236 (+0.9%)
~~POC~~Particulate Organic Carbon ($\times 10^9$ mol C)	22.7	22.4 (-1.3%)	19.9 (-12.3%)
NPP (mmol N m^{-2} d^{-1})	4.65	3.92 (-15.7%)	3.57 (-23.2%)
New Production + Regeneration Production (mmol N m^{-2} d^{-1})	2.83+1.82	2.21+1.71 (-21.9%, -6.0%)	1.82+1.75 (-35.7%, -3.8%)
Fluxes			
Vertical NO_3 flux across 100 m level ($\times 10^9$ mol d^{-1}, positive upward)	0.2454	0.1313 (-46.5%)	0.0011 (-99.6%)
Top 100 m integrated zonal NO_3 flux across 109° E section* ($\times 10^9$ mol d^{-1}, positive westward)	0.4156	0.2652 (-36.2%)	0.2013 (-51.6%)
Vertical volume flux across 100 m level (Sv, positive upward)	0.22	0.14 (-36.4%)	0.04 (-81.8%)
Top 100 m integrated zonal volume flux across 109° E section* (Sv, positive westward)	0.44	0.01 (-97.7%)	0.28 (-36.4%)

*** See Fig. 11a for the location.**

Figures

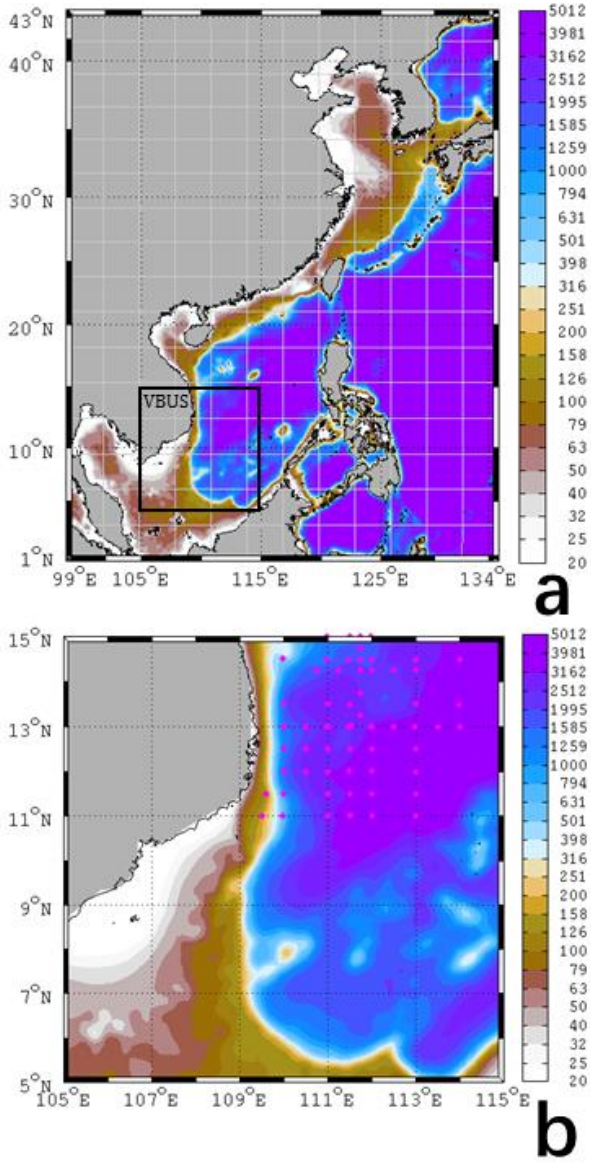
43°N
40°N
30°N
20°N
10°N
1°N
99°E
105°E
115°E
125°E
134°E
VBUS
5012
3981
3162
2512
1995
1585
1259
1000
794
631
501
398
316
251
200
158
126
100
79
63
50
40
32
25
20
a
15°N
13°N
11°N
9°N
7°N
5°N
105°E
107°E
109°E
111°E
113°E
115°E
b

655

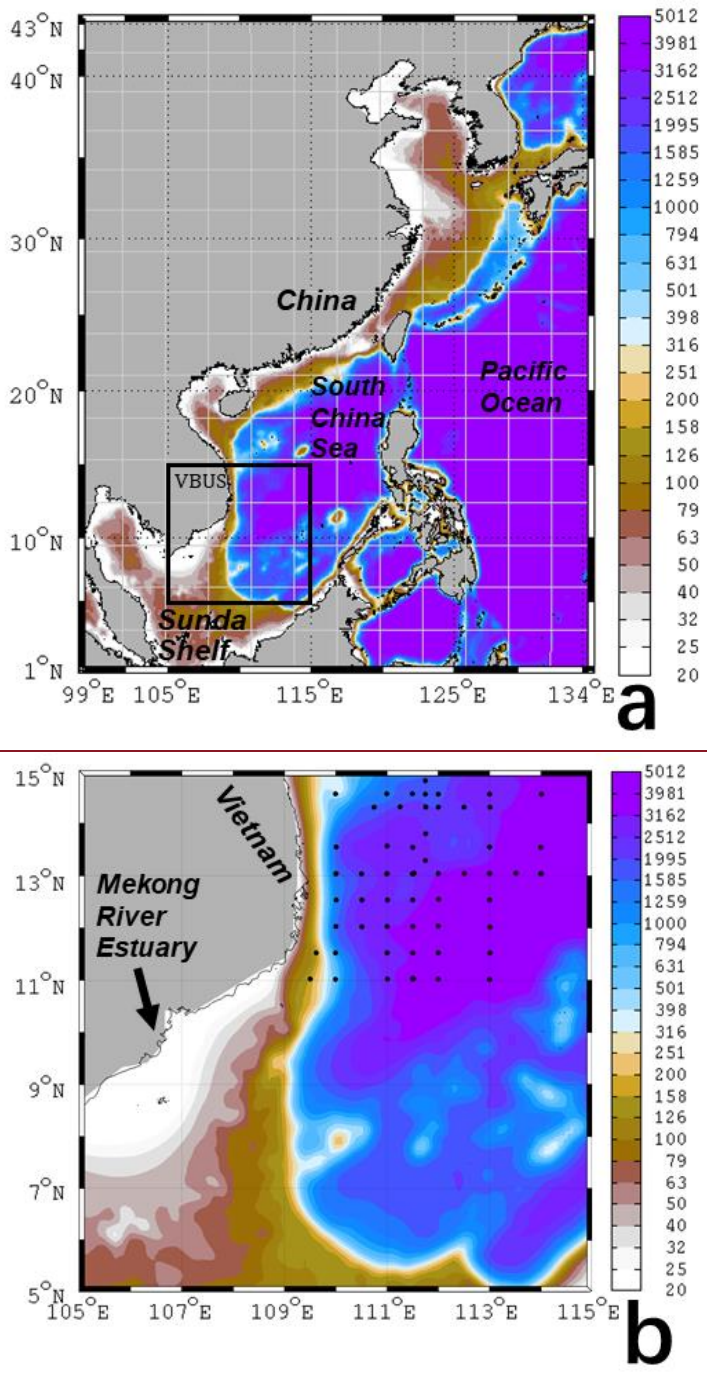

Figure 1 (a) Model domain and the bathymetry (unit: meter) for the TFOR-CoSINE model. Model grid nodes are shown every 25 points. The study area VBUS is boxed. (b) Zoom-in area of VBUS. ~~Magenta~~Black diamonds are the observation stations (see text).

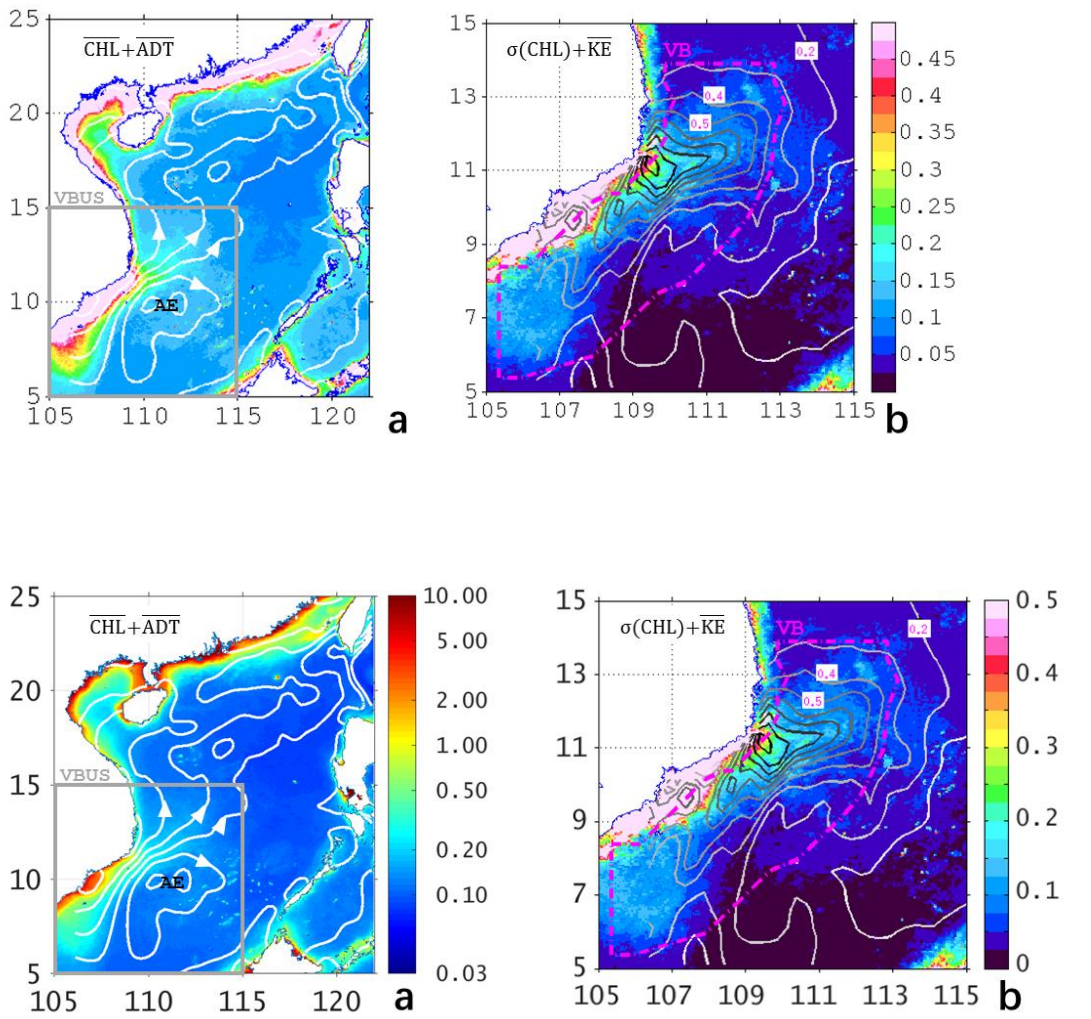

Figure 2 (a) Summertime (MJJAS) average of surface ~~CHL~~ chlorophyll concentration (color shading, unit: mg m^{-3}) from MODIS, overlapped white contours are mean ADT with the arrows showing the directions of geostrophic currents. Gray box is the region of interest (VBUS), while AE shows the center of the anticyclone. (b) Standard derivation of surface ~~CHL~~ chlorophyll (color shading, unit: mg m^{-3}) overlapped with the contours of surface KE with an interval of 0.1 from 0.1 to 1.0 (unit: m^2 s^{-2}). ~~Magenta box is the box region~~ The magenta dot-dash contour delimits the ocean region over which chlorophyll and KE are averaged (see text).

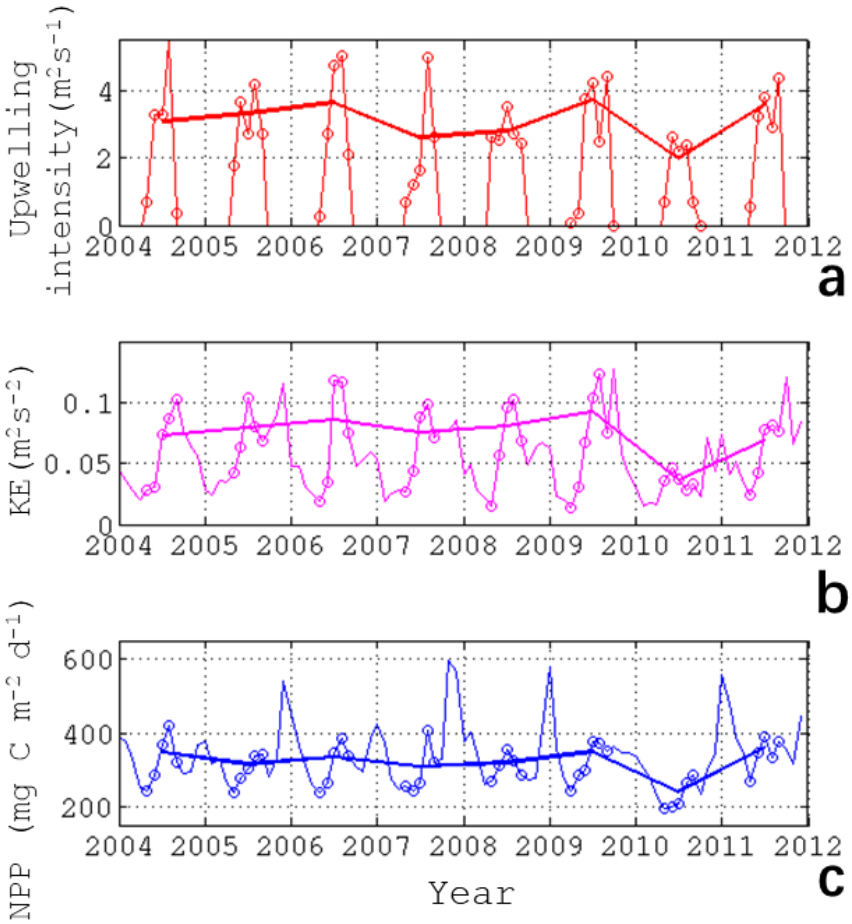
Upwelling intensity(m²s⁻¹)
0
2
4
2004 2005 2006 2007 2008 2009 2010 2011 2012
a
KE(m²s⁻²)
0
0.05
0.1
2004 2005 2006 2007 2008 2009 2010 2011 2012
b
NPP (mg C m⁻² d⁻¹)
200
400
600
2004 2005 2006 2007 2008 2009 2010 2011 2012
Year
c

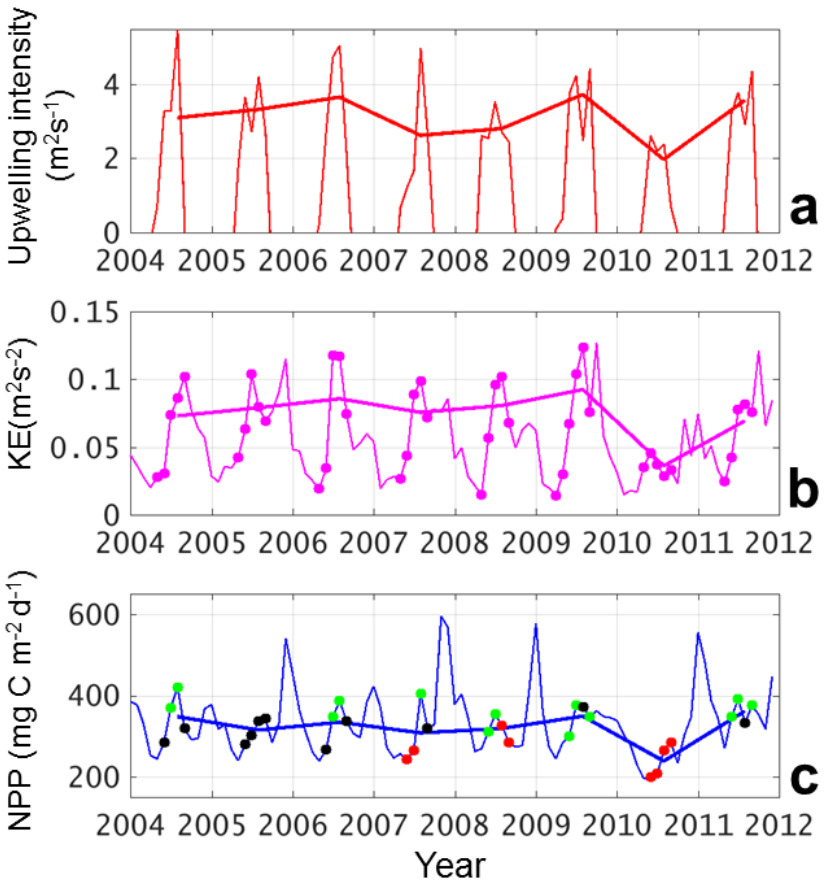

Figure 3 Time series of (a) UI in m^2 s^{-1}, (b) KE in m^2 s^{-2} and (c) NPP in mg C m^{-2} d^{-1} of monthly data (thin lines) and summer mean (thick lines). In (a), only the positive (upwelling-favorable) values are shown. ~~Months~~In (b), months with positive UI are marked with ~~open circles.~~dots. In (c), green, black and red dots indicate HNA, normal and LNA scenarios (see text for definition).

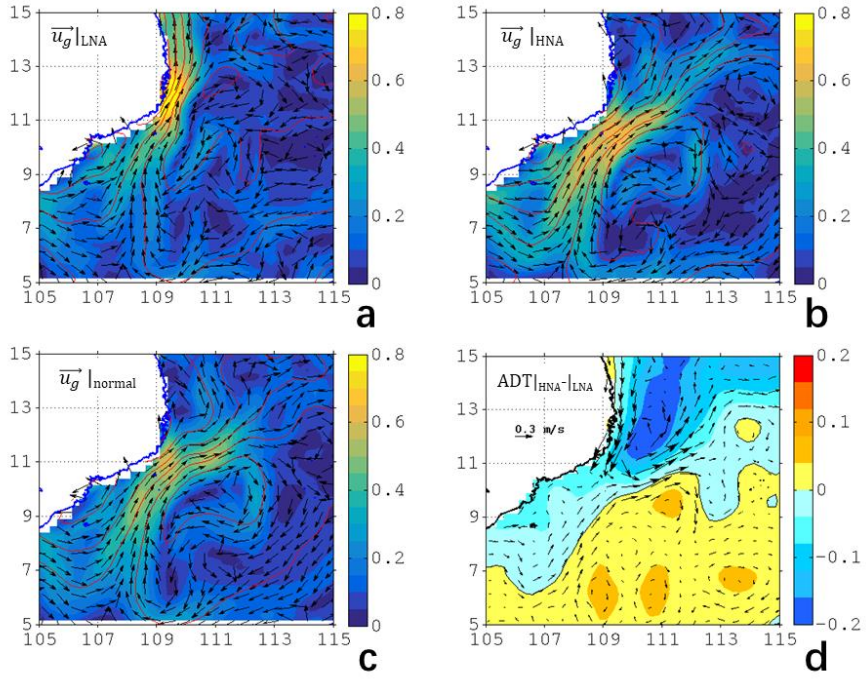

Figure 4 The surface geostrophic current velocity (color shading, unit: m s^{-1}), direction (vectors), and respective ADT (red contours, unit: meter) in (a) LNA ~~(a),~~ (b) HNA ~~(b),~~ and (c) normal months (i.e., neither LNA nor HNA~~, c~~) scenarios (see text for criteria). (d) The differences of ADT and geostrophic current between HNA and LNA.

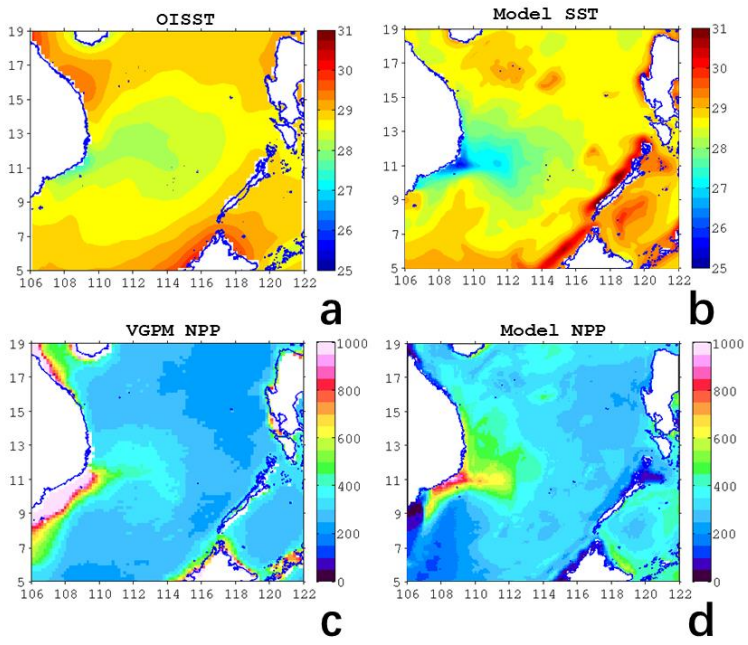

Figure 5 (a) OISST and (b) model SST (unit: °C), (c) VGPM NPP and (d) modeled NPP (unit: mg C m^{-2} d^{-1}) in multi-year August average.

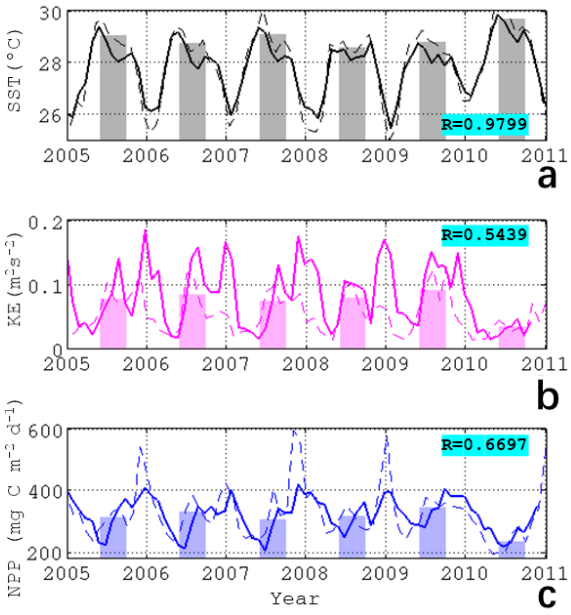
SST (°C)
30
28
26
R=0.9799
2005
2006
2007
2008
2009
2010
2011
a
KE (m²s⁻²)
0.2
0.1
0
R=0.5439
b
NPP (mg C m⁻² d⁻¹)
600
400
200
R=0.6697
Year
c

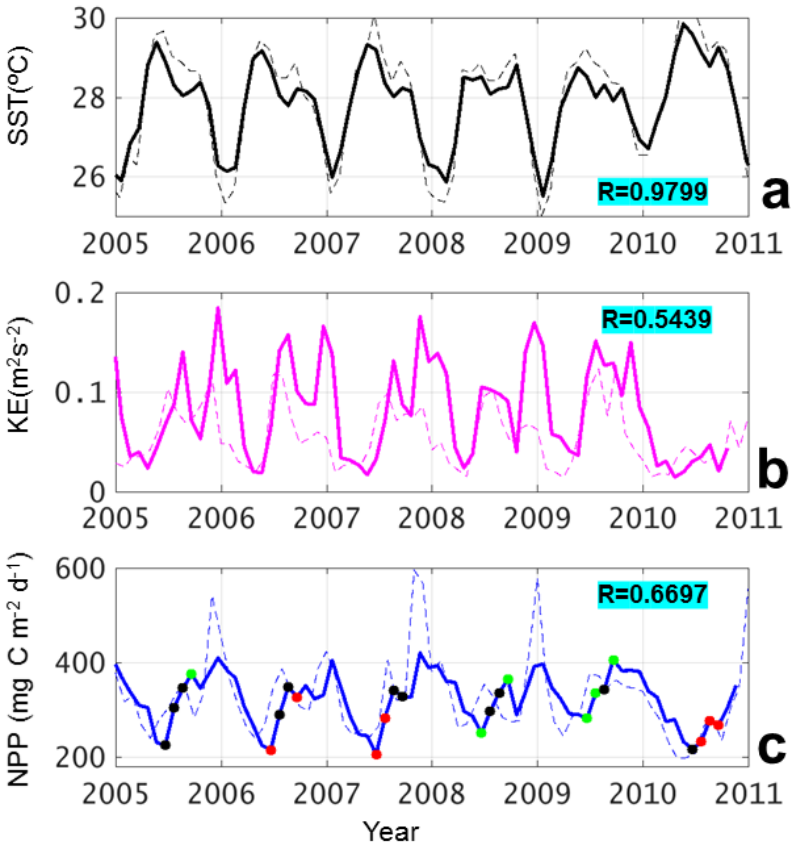

Figure 6 Thick lines: modeled (a) SST in °C, (b) KE in $m^2 s^{-2}$, and (c) NPP in mg C $m^{-2} d^{-1}$ averaged over the box region (see Fig. 2b), with respective observation data (thin dashed lines~~) and their summer mean (bar).~~). Correlation coefficients are also show in each plot. In (c), green, black and red dots indicate HNA, normal and LNA scenarios (see text for definition).

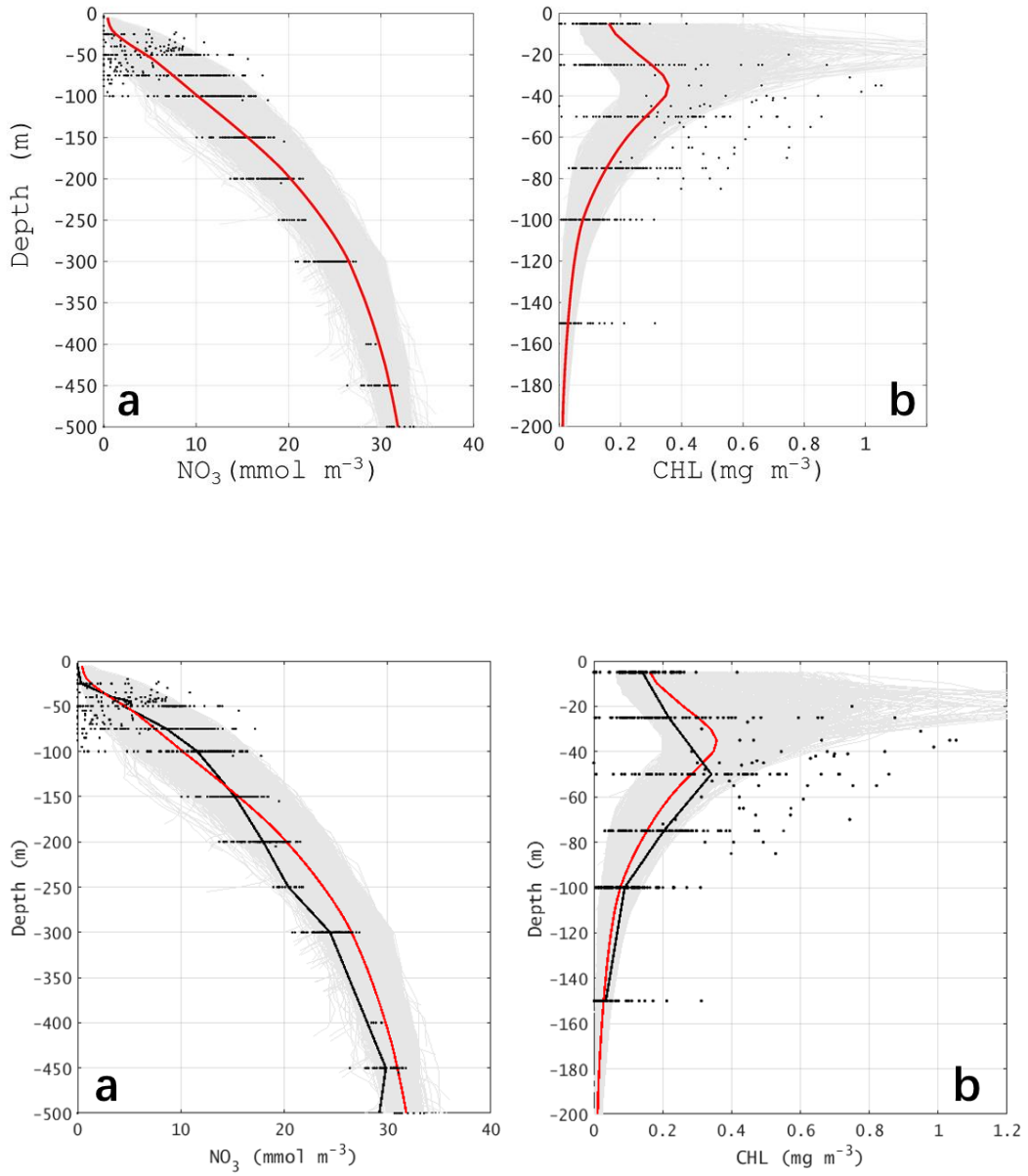

Figure 7 The vertical profiles of (a) nitrate concentration (unit: mmol m^{-3}) and (b) ~~CHL~~chlorophyll concentration (unit:mg m^{-3}). In both plots, the black dots are the observation values (see Fig. 1b for stations). The gray area are the envelop for all model stations in the same area and month, while the red lines are the area-mean profiles.

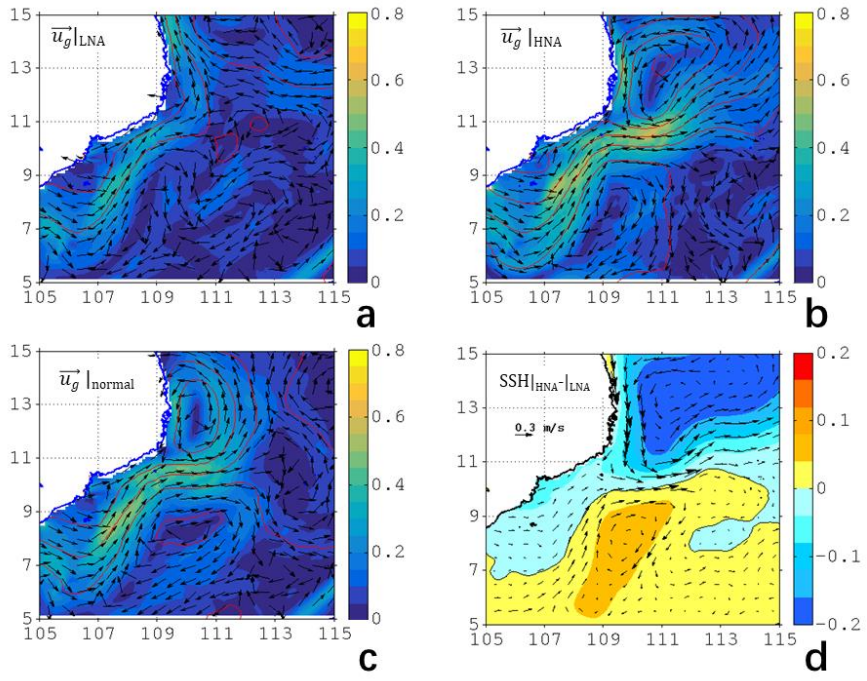

Figure 8 Same with Fig. 4, but based on model outputs.

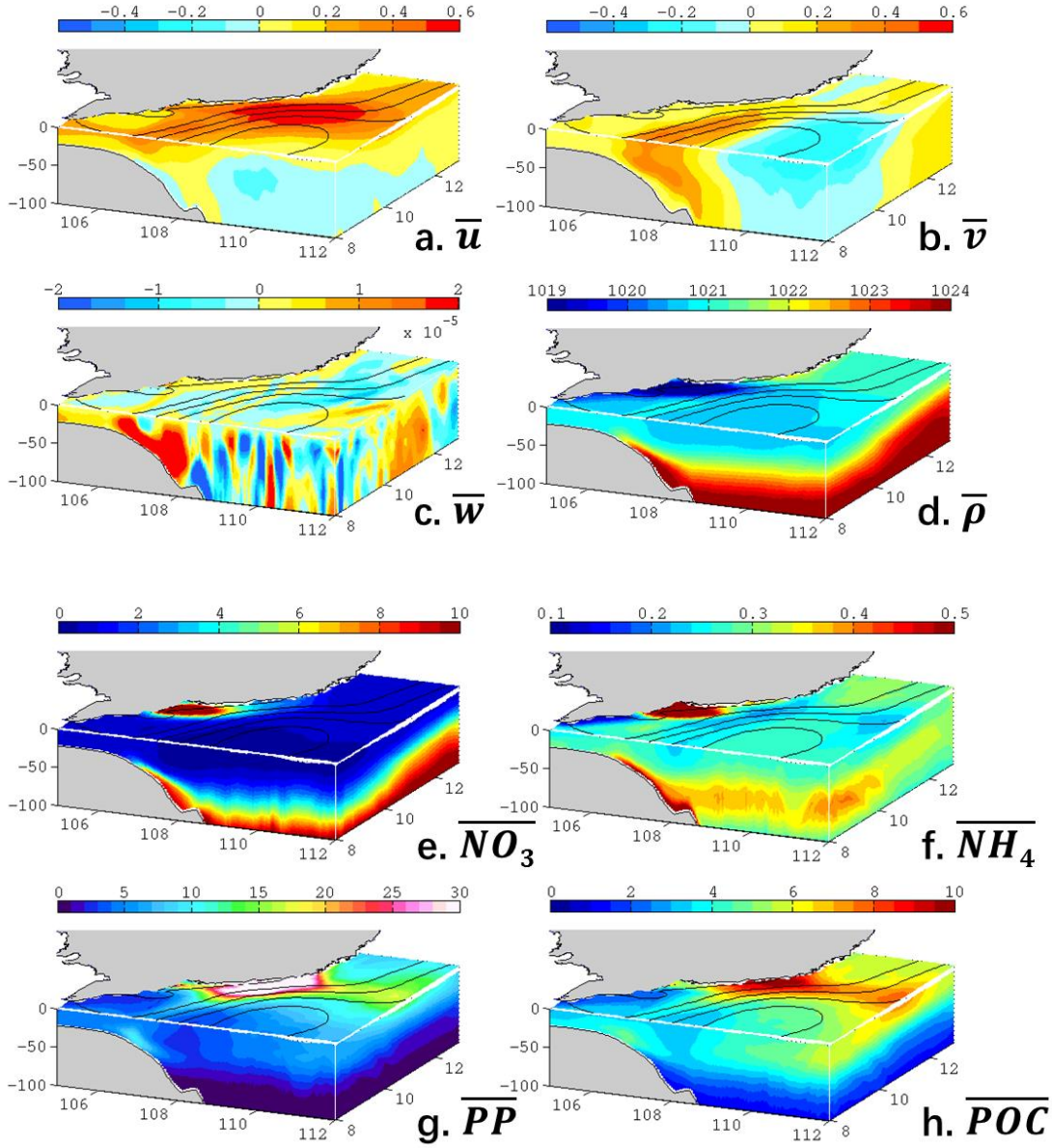

Figure 9 Three-dimensional distribution (standard run) of the summer mean (a) zonal velocity in m s^{-1}, (b) meridional velocity in m s^{-1}, (c) vertical velocity in m s^{-1}, (d) potential density in kg m^{-3}, (e) nitrate in mmol m^{-3}, (f) ammonium in mmol m^{-3}, (g) primary production in mg C m^{-3} d^{-1}, and particulate organic carbon in mmol C m^{-3}. Overlapped contours are the mean sea level (every 0.1 m).

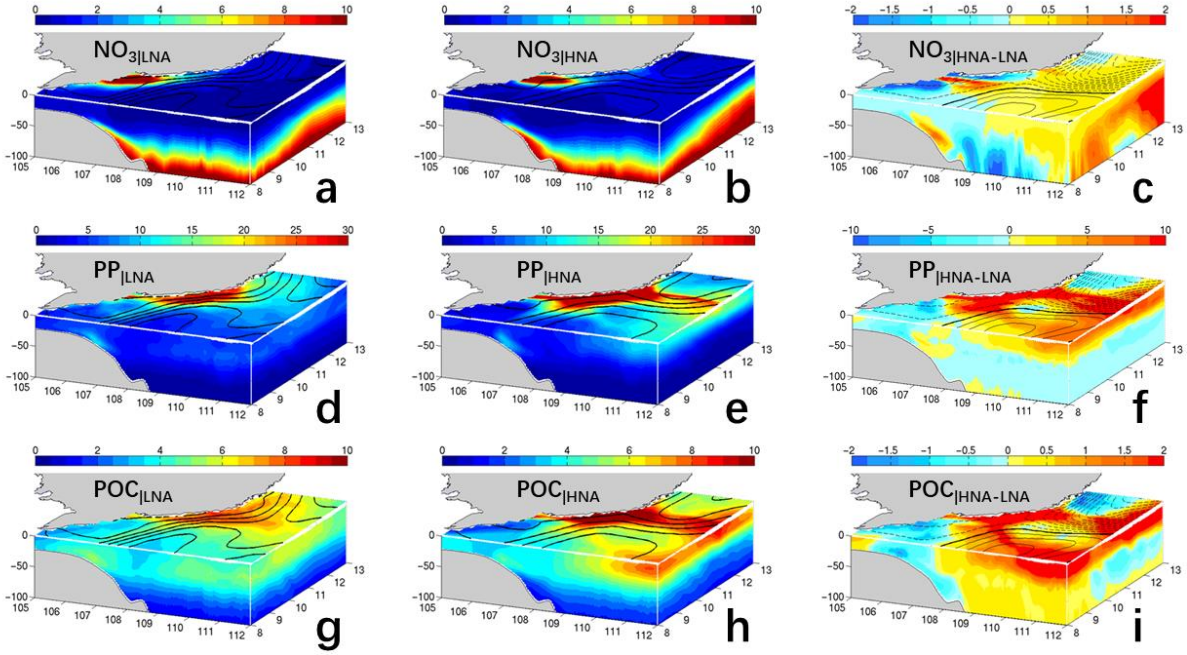

Figure 10 Modeled NO_3 (first row, in mmol m^{-3}), PP (second row, mg C m^{-3} d^{-1}) and ~~POC~~particulate organic carbon (third row, mmol C m^{-3}) distribution in LNA (left column), HNA (middle column) and the difference between two scenarios (right column). See text for the defination of LNA and HNA.

715

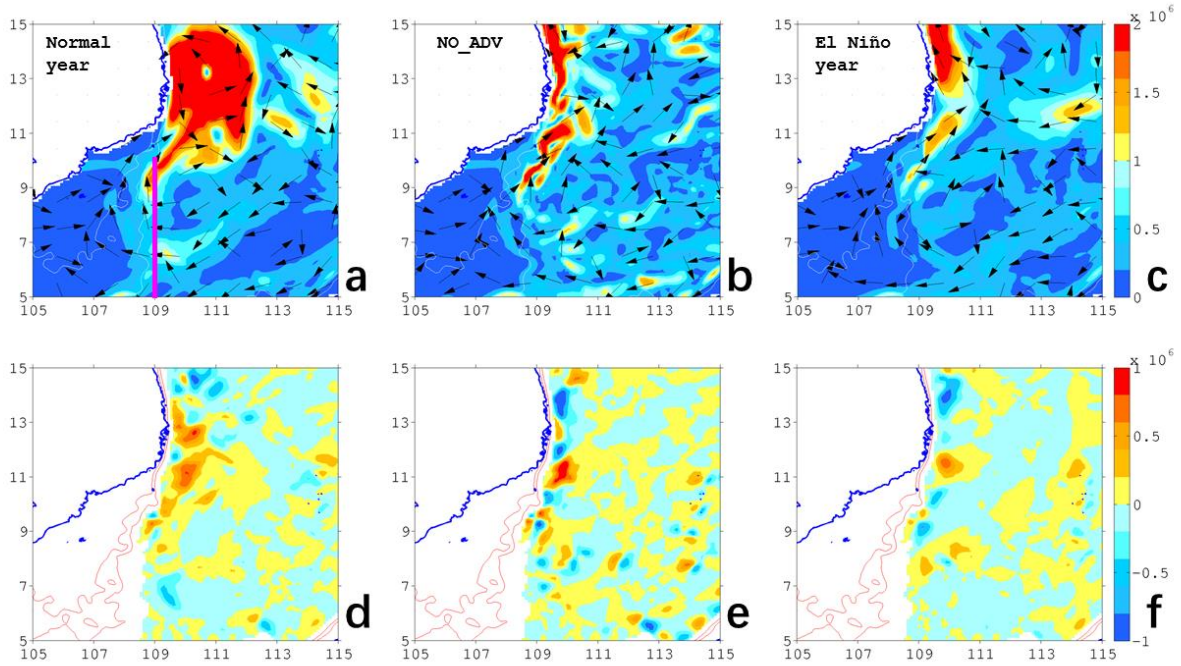

Figure 11 (Upper) Modeled 0-100 m integrated nitrate fluxes (unit: mmol s^{-1}) in horizontal plane. Color shading is the magnitude while vectors denote the direction. (Lower) Vertical flux across 100 m level for normal year (a and d, years other than 2010), NO_ADV case (b and e), and post-El Niño (c and f, in year 2010). Overlapped contours are the 50 m and 75 m isobath. In (a), the magenta line is the 109° E section (Table 1).

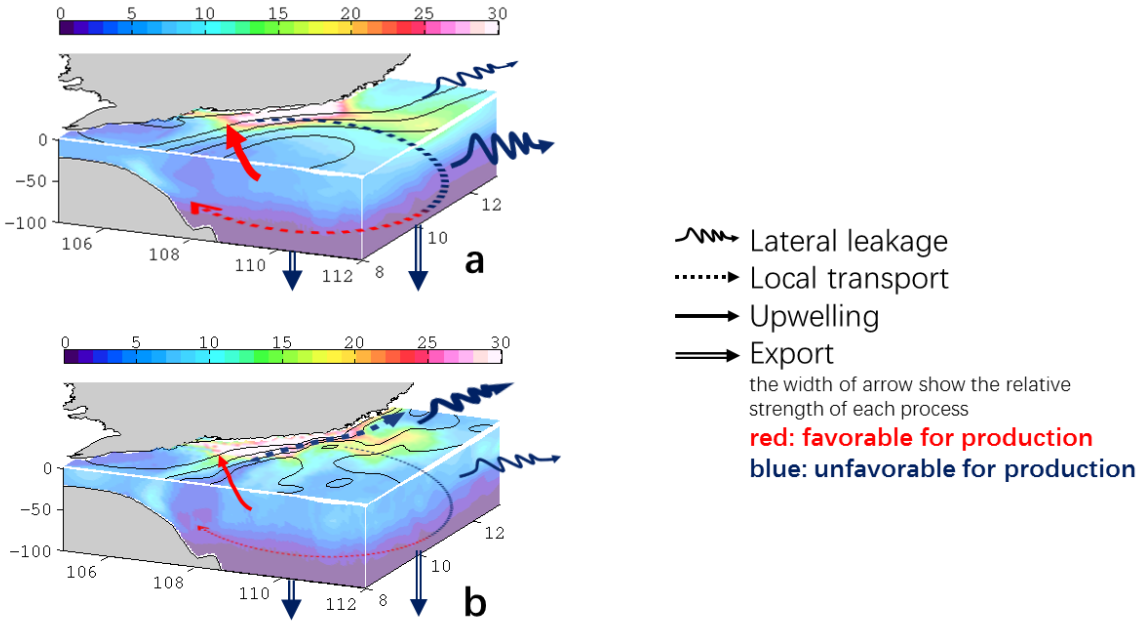

Figure 12 Schematic diagram summarizing the dynamics in different scenarios of distinct circulation pattern in the VBUS, overlapped with the three-dimensional distribution of PP (unit: mg C m^{-3} d^{-1}). (a) Normal state: The separated jet transports the upwelled nutrient and produced organic matter offshore. While a substantial portion of the offshore transported organic matter leaks into the interior of SCS and never comes back, the recirculation and quasi-stationary anticyclonic eddy trap the organic matters locally, and hinder further leakage of available nutrients in VBUS. The locally recirculated nutrient is then upwelled in the bottom Ekman layer, rejoining the production process over the shelf. (b) Non-separation state: During the non-separated circulation, the along-isobath circulation transports the organic matter northward. The leakage of organic matter reduces the nutrient inventory in the VBUS. The loss of nutrients diminishes the nutrient inventory available for remineralization and upwelling, further inducing a reduction in the production process.